I.S. Office of Naval Research
407-C

NAVAL RESEARCH REVIEWS

JULY 1978

DEPARTMENT OF THE NAVY · OFFICE OF NAVAL RESEARCH
OCT 10 1978
The University of Michigan Engineering Library

UNIVERSITY OF MICHIGAN LIBRARIES
SEP 28 1978
DEPOSITED BY THE UNITED STATES OF AMERICA
THE UNIVERSITY OF MICHIGAN
OCT 12 1978
ENGINEERING
Digitized by Google
Original from UNIVERSITY OF MICHIGAN
Generated for member (University of Maryland, College Park) on 2014-10-01 20:21 GMT / http://hdl.handle.net/2027/mdp.39015047405512
Public Domain, Google-digitized / http://www.hathitrust.org/access_use#pd-google

PROFILES IN SCIENCE

Dr. William R. Sears

Dr. William R. Sears is Professor of Aerospace and Mechanical Engineering at the University of Arizona. In the field of fluid mechanics he is well known for his studies of unsteady airfoil theory, including gust effects. His recent discovery of the nature of boundary layer separation in unsteady flows is among his major accomplishments. His research has led to a better understanding of wings in unsteady motion, supersonic flow about projectiles, and magnetohydrodynamics. Presently he is working under contract to the Office of Naval Research studying controllable — wall wind tunnels to reduce, significantly, wall interference at transonic speeds.

Professor Sears is a member of the National Academy of Sciences and the National Academy of Engineering and has served on the Naval Research Advisory Committee. In 1974 he was awarded the German "Prandtl Ring."

Digitized by Google

Original from UNIVERSITY OF MICHIGAN

Generated for member (University of Maryland, College Park) on 2014-10-01 20:21 GMT / http://hdl.handle.net/2027/mdp.39015047405512
Public Domain, Google-digitized / http://www.hathitrust.org/access_use#pd-google

Analysis of Advanced Variable Camber Concepts for Combat Aircraft*

R.F. Siewert
Naval Air Systems Command

and

R.E. Whitehead†
Office of Naval Research

Introduction

Since Horatio Frederick Phillips [1] filed a patent in 1884 for an airfoil demonstrating superior lift capability due to drooping the leading edge, aircraft designers have been struggling with the problem of optimizing the airfoil design to operate efficiently throughout the flight envelope. A typical mission for combat aircraft involves a number of different flight conditions: There are take-offs and landings at which high lift at relative low speed is required; the cruise to the combat arena may require moderate lift at moderate speeds and altitudes with the minimum drag possible; depending on the combat mission the aircraft may be required to fly supersonically and/or to maneuver quickly at transonic or high subsonic speeds. The optimum wing planform and section profile will be different for each of the mission flight conditions. Therefore, the final wing design is typically a compromise of these optimums. The basic configuration

---

*From a paper presented by the authors at the AGARD Multi-Panel Symposium on Fighter Aircraft Design, Florence, Italy, October 1977.

†Dr. Whitehead is the Scientific Officer for Aerodynamics and Hydromechanics in the Vehicle Technology Program for ONR. His research has been primarily in the field of computational fluid mechanics.

Mr. Siewart is the Technology Administrator for Aerodynamics in the Naval Air Systems Command. He has been instrumental in the development of many new aerodynamic concepts to benefit naval aviation.

Digitized by Google

Original from UNIVERSITY OF MICHIGAN

Generated for member (University of Maryland, College Park) on 2014-10-01 20:21 GMT / http://hdl.handle.net/2027/mdp.39015047405512
Public Domain, Google-digitized / http://www.hathitrust.org/access_use#pd-google

meets some "design point" performance criteria at one flight condition with some less than optimum performance at other "off design" flight conditions. A combat aircraft is designed primarily for combat; any maneuvers not concerned with combat are referred to as "off design" flight conditions. It is the use of various concepts to employ variable camber to obtain near optimum wing section configurations for all flight conditions that is the subject of this article. Camber in the context of airfoils refers to the curvature of the airfoil section about the chord, which is a straight line connecting the airfoil leading and trailing edges. Camber is one of the most important parameters affecting the lifting characteristics of wings. The concept of varying camber in flight to alter the lift characteristics is not new. The Wright Brothers employed variable camber through wing warping to obtain lateral control of the first successful airplane. Increasing the camber of the wing to achieve increased lift for take-off and landing has been common practice since the 1920's; however, the concept of improving the "off design" performance, particularly during the midmission phases of flight, is a more recent application of this technology. It was found that subsonic cruise performance could be enhanced through partial deflection of the variable camber leading edge devices used in landing with the design of very thin wings for supersonic flight. Continued efforts to increase the maneuvering performance of combat aircraft subsequently have lead to numerous variable camber concepts specifically oriented to this goal. It is this application of variable camber, namely increased transonic maneuverability and off-design performance that will be addressed in this paper.

Variable camber devices have taken many forms over the years. Concepts have varied from plain flaps on the leading and trailing edges of the wing to the more sophisticated leading edge slat designs. Recent advances in materials technology and innovative mechanical design concepts have provided the capability of smoothly varying camber with no discontinuities in the wing surface. This paper is concerned only with devices that vary camber by deflecting the leading and trailing edges of the wing. Other variable geometry concepts such as variable sweep and extendable strakes, although important in their own right in aircraft performance, are not considered in the present analysis.

A review is presented of the applications of variable camber to enhance maneuverability on contemporary combat aircraft. This is followed by a survey of the more recent variable camber concepts under study. While this survey is intended to be comprehensive, it is recognized that it is far from all inclusive. New concepts are constantly evolving and it is all but impossible to keep abreast of all new

Generated for member (University of Maryland, College Park) on 2014-10-01 20:21 GMT / http://hdl.handle.net/2027/mdp.39015047405512
Public Domain, Google-digitized / http://www.hathitrust.org/access_use#pd-google
Digitized by Google
Original from
UNIVERSITY OF MICHIGAN

developments. Finally, analysis is presented to describe the benefits obtainable through the application of variable camber, at least to first order. This analysis is intended to provide some general observations as to what increases in complexity and structural weight can be tolerated without negating the improved aerodynamic performance of the various devices.*

Current Applications of Variable Camber

In reviewing the application of variable camber concepts to contemporary aircraft in order to improve maneuverability, two basic approaches become apparent. The first is to retrofit variable camber devices on an existing aircraft with a demonstrated deficiency, while the second is the development of a new aircraft which considers variable camber to be an integral part of the design from the outset. The latter approach usually results in automatic or semi-automatic operation of the variable camber as a function of flight condition.

Probably the best known recent application of the first approach of variable camber to improve transonic maneuverability is that of the maneuvering slats on the F-4E aircraft. Very similar flaps, with improved low speed characteristics will also be retrofitted on the U.S. Marine Corps F-4J aircraft which will be designated the F-4S. The objectives of the F-4E leading edge slat application was to increase the angle-of-attack for buffet onset and consequently increase the maneuvering lift coefficient. These slats were the subject of extensive wind tunnel and flight test evaluation [2]. Based on wind tunnel data (Figure 1) this configuration did increase the buffet onset angle-of-attack from 7.0° to 10.6° with a corresponding increase in maneuver lift coefficient of approximately 0.2 at 0.8 Mach number (the ratio of vehicle speed to the local speed of sound.) These wind tunnel tests were confirmed during subsequent flight tests.

Later models of the F-14A aircraft will employ leading edge slats in conjunction with trailing edge flaps. Because of the automatic wing sweep features of the F-14A, the variable camber devices, particularly the trailing edge flaps, must be retracted prior to 0.9 Mach number. Consequently the F-14A variable camber is designed to improve maneuvering performance at the low to mid transonic speed

*The authors wish to express their appreciation to Mr. Lynn Trobaugh of the David Taylor Naval Ship Research and Development Center for his assistance in modifying the mission analysis code and obtaining the performance data that is presented.

Generated for member (University of Maryland, College Park) on 2014-10-01 20:21 GMT / http://hdl.handle.net/2027/mdp.39015047405512
Public Domain, Google-digitized / http://www.hathitrust.org/access_use#pd-google
Digitized by Google
Original from
UNIVERSITY OF MICHIGAN

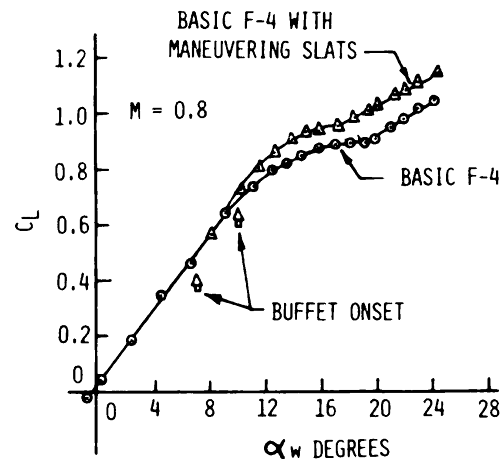

Figure 1 — Effect of F-4E maneuver slats on buffet onset

range. The F-14A variable camber system is designed to be automatic, with deployment of the devices being a function of flight condition; therefore, the variable camber drag polars (Figure 2) represent an optimum envelope of several configurations. As can be seen from the data, there is a cross over at approximately 0.85 lift coefficient at both Mach numbers where the clean wing demonstrates greater aerodynamic efficiency, indicating the basic F-14A wing was designed to possess more than the minimum maneuver capability. This crossover, which is typical of slatted configurations, points up one of the problems of retrofit applications of variable camber; that is, less than the maximum performance is obtained from the devices for some flight conditions and a penalty might have to be paid in other flight regimes because the basic wing was designed to have some maneuver capability.

Other aircraft, the F-5E for example, employ variable camber in the form of plain leading and trailing edge flaps that were part of the initial design. The F-5E application is termed semi-automatic in that the pilot selects a predetermined flap deflection as a function of flight condition. The F-5E is characteristic of other aircraft, in that the maneuverability improvements due to variable camber are reduced significantly approaching 0.9 Mach number.

The YF-16 aircraft was designed almost from the outset to utilize variable camber [3]. In this aircraft, the variable camber consists of automatically deflecting plain leading edge flaps as a function of flight condition. At 0.8 Mach number, the automatic variable camber increases sustained turn capability 18% (Figure 3) over that obtained with the basic wing which was designed to yield maximum left/drag at cruise.

Digitized by Google
Original from
UNIVERSITY OF MICHIGAN
Generated for member (University of Maryland, College Park) on 2014-10-01 20:21 GMT / http://hdl.handle.net/2027/mdp.39015047405512
Public Domain, Google-digitized / http://www.hathitrust.org/access_use#pd-google

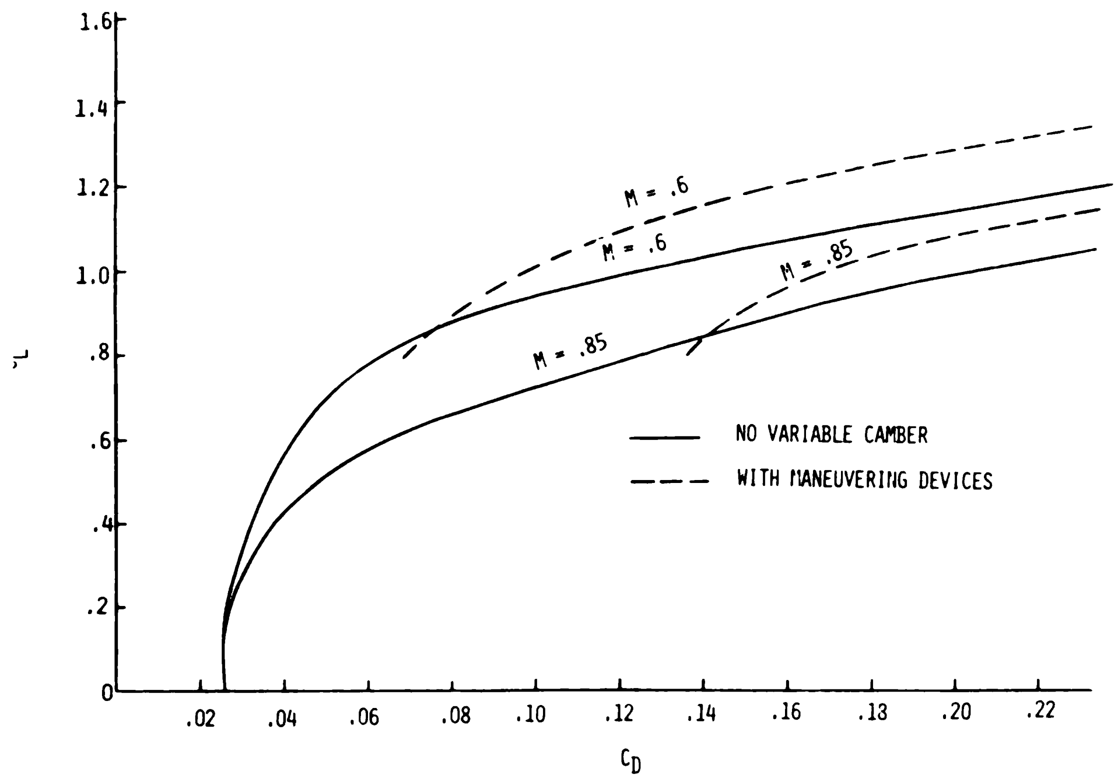

Figure 2 — F-14A drag polars

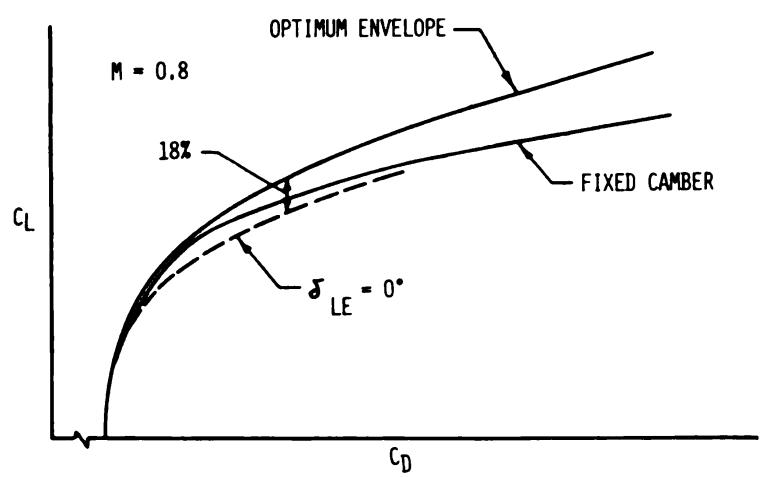

Figure 3 — YF-16 improved lift/drag due to leading edge deflection

Generated for member (University of Maryland, College Park) on 2014-10-01 20:21 GMT / http://hdl.handle.net/2027/mdp.39015047405512
Public Domain, Google-digitized / http://www.hathitrust.org/access_use#pd-google
Digitized by Google
Original from
UNIVERSITY OF MICHIGAN

The U.S. Navy F-18 aircraft is also being designed to exploit variable camber for improved maneuverability [4]. The F-18 system is to be automatic and follows a rather complex deployment schedule. Significant improvements in maneuverability accrue for representative maximum turn rate levels of drag at 0.6 and 0.8 Mach number; however, the improvement in maneuver capability at 0.9 Mach number has been considerably reduced. This significant decrease in improvement due to variable camber at 0.9 Mach number was also noted for the YF-16. [3]

It appears that fighter aircraft maneuver enhancement, through the application of leading and trailing edge variable camber concepts, has gained wide spread acceptance. The "off design" benefits to accrue from the use of variable camber are greater, if the concept is considered in the initial design phases of a new aircraft, rather than applied as an "add-on" later.

Advanced Variable Camber Concepts

An extensive study of the application of conformally varying camber to fighter/attack configurations was conducted for the Office of Naval Research [5]. A detailed analytical and experimental investigation was performed to assess the potential of variable camber for improving combat performance. The basic aircraft chosen for the study was the Navy F-8. The F-8 is a single seat fighter designed in the 1950's with supersonic capability. The F-8 was chosen as the baseline aircraft because of its performance characteristics and because the wing on the F-8 could be readily replaced with a variable camber wing for flight demonstration, which was an original long term objective of the program.

A new advanced technology wing (ATW) was designed as the basic variable camber wing. The wing planform was basically the same as the F-8 wing, however, the airfoil sections used for the new wing were of the thin supercritical type with a "peaky" pressure distribution (Figure 4). To achieve variable camber the wing was designed to have smoothly variable sections between 5% and 25% chord and between 72.5% and 90% chord. With these airfoil sections, the new wing had, as might be expected, very good cruise and loiter characteristics.

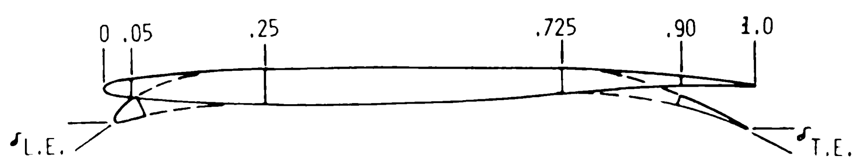

Figure 4 — Advanced technology wing, airfoil section

Generated for member (University of Maryland, College Park) on 2014-10-01 20:21 GMT / http://hdl.handle.net/2027/mdp.39015047405512
Public Domain, Google-digitized / http://www.hathitrust.org/access_use#pd-google
Digitized by Google
Original from UNIVERSITY OF MICHIGAN

An experimental program was conducted on a 1/10 scale model of the F-8 both with the basic and advanced technology wing. For the test, 6 leading edge and 5 trailing edge conformal flap deflections were fabricated. In addition, plain hinged leading and trailing edge flaps were fabricated and tested on the advanced technology wing for comparison. Wind tunnel tests were conducted in the Mach range from 0.2 to 2.0 at the NASA Ames Research Center.

Based on the experimental data and existing F-8 data, performance comparisons were made between the basic F-8 with and without leading edge droop and the advanced technology wing with both plain and conformal leading and trailing edge flaps. As one would expect, the newly designed advanced technology wing shows significant performance improvements over the basic F-8 wing at subsonic free stream mach numbers even without leading and trailing edge flaps, either conformal or plain. The most interesting comparison is the one between the advanced wing with plain flaps and with conformal variable camber (Figures 5 and 6). In this case, at a C_L of 0.8 and mach numbers of 0.7 and 0.9 the conformal camber shows respective decreases in drag of 18% and 6% compared to the plain flaps. In addition to reduced drag, the maximum useable lift coefficient is greater for the advanced technology wing with conformal camber than with plain flaps for every Mach number tested (Figure 7). Maximum useable lift was defined by taking an increment in angle-of-attack above buffet onset which was determined by force and moment variation and trailing pressure.

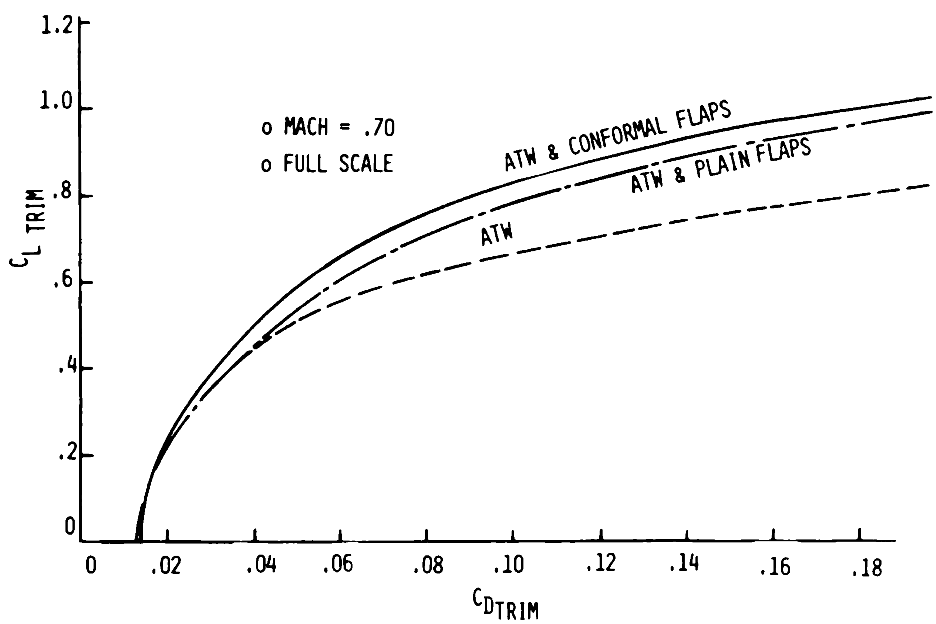

Figure 5 — Advanced technology wing-drag polars

Generated for member (University of Maryland, College Park) on 2014-10-01 20:21 GMT / http://hdl.handle.net/2027/mdp.39015047405512
Public Domain, Google-digitized / http://www.hathitrust.org/access_use#pd-google
Digitized by Google
Original from UNIVERSITY OF MICHIGAN

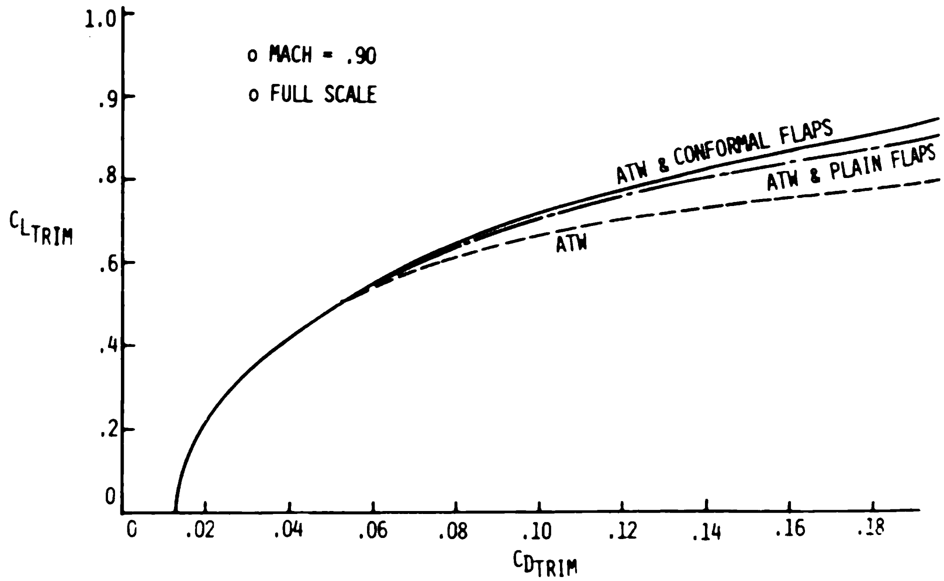

Figure 6 — Advanced technology wing — drag polars

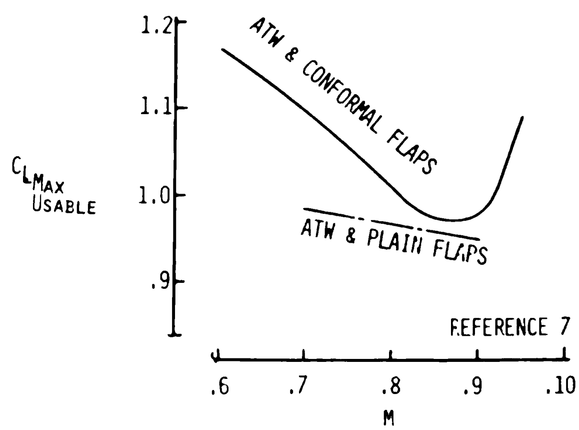

Figure 7 — Advanced technology wing — maximum useable lift

At supersonic freestream Mach numbers, a condition closer to that for which the F-8 wing was designed, the advanced technology wing has a higher drag coefficient at every lift coefficient. At a Mach number of 2.0, for instance, the zero lift drag is 13% less for the basic F-8 than for the advanced technology wing. This should be expected for the supercritical type airfoil with a rather large leading edge radius used for the advanced technology wing. Neither the conformal nor plain flap can be used to advantage for this flight condition, although a slight negative deflection of the plain flap improves the drag slightly. The higher drag for supersonic mach numbers should not necessarily reflect negatively on either conformal variable camber or plain flaps; however, if the larger leading

Generated for member (University of Maryland, College Park) on 2014-10-01 20:21 GMT / http://hdl.handle.net/2027/mdp.39015047405512
Public Domain, Google-digitized / http://www.hathitrust.org/access_use#pd-google
Digitized by Google
Original from
UNIVERSITY OF MICHIGAN

edge radius becomes necessary to the concept and if the aircraft mission contains a sizeable supersonic dash, then the advantages at cruise, loiter, and maneuver conditions would have to be traded off against the supersonic penalty.

Performance comparisons in reference 7 for the advanced technology wing with conformal and plain flaps are what one would expect from the data. The lower drag for the conformal flaps results in better performance during cruise and loiter and better combat fuel flow at a given maneuvering load factor. These performance comparisons do not include any supersonic dash mission segments for which the advanced technology wing would have to pay a drag penalty.

Segmented Variable Camber

A unique variable camber concept has been developed with Naval Air Systems Command support in which the leading and trailing edge flaps are divided into four segments, with the hinge line skewed, i.e., not aligned with a constant chord element (Figure 8). The result is a wing which displays basically conical camber, with the capability to vary camber of the leading and trailing edges independently through a wide variation of shapes. This concept has been tested by the NASA [6] and an analysis of the potential benefits of the application of the sytem on a conceptual fighter aircraft have been reported [7].

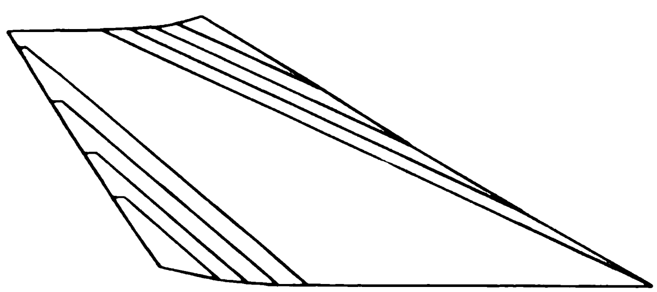

Figure 8 — Segmented variable camber wing

A firm conclusion of the study is that even with a weight penalty of 1000 lbs. required to implement the variable camber concept, buffet free sustained load factors 50 to 60 percent greater than those obtained for aircraft configurations with an uncambered or a fixed camber wing are achievable. The study further concludes that the principal advantage of this variable camber concept at 0.9 Mach number is the improvement in wing buffet onset lift coefficient, but at the expense of increased aircraft drag. This concept does have the additional flexibility that with the skewed hinge lines variable camber and spanwise twist distribution are both achieved simultaneously.

Generated for member (University of Maryland, College Park) on 2014-10-01 20:21 GMT / http://hdl.handle.net/2027/mdp.39015047405512
Public Domain, Google-digitized / http://www.hathitrust.org/access_use#pd-google
Digitized by Google
Original from UNIVERSITY OF MICHIGAN

The previous concepts had no provision for spanwise variation of camber.

Self-Optimizing Wing Concept

A somewhat different application of conformal variable camber has been investigated under sponsorship of the Navy and Air Force. The goal of the investigation is to develop a flexible wing/digital computer wind tunnel model system that will automatically optimize the wing configuration for a specified set of flight conditions. In operation, the digital computer is loaded with a gradient projection optimization code which takes force and moment data from the wind tunnel balance system and predicts model configuration changes to optimize the desired aerodynamic parameters. The model is built with flexible panels and internal actuators which permit changes in camber, twist, leading edge radius and thickness distributions while maintaining a smooth wing contour. The computer commands, through the control system, changes to the wing geometry based on the optimization predictions to optimize the desired parameters within given constraints (Figure 9).

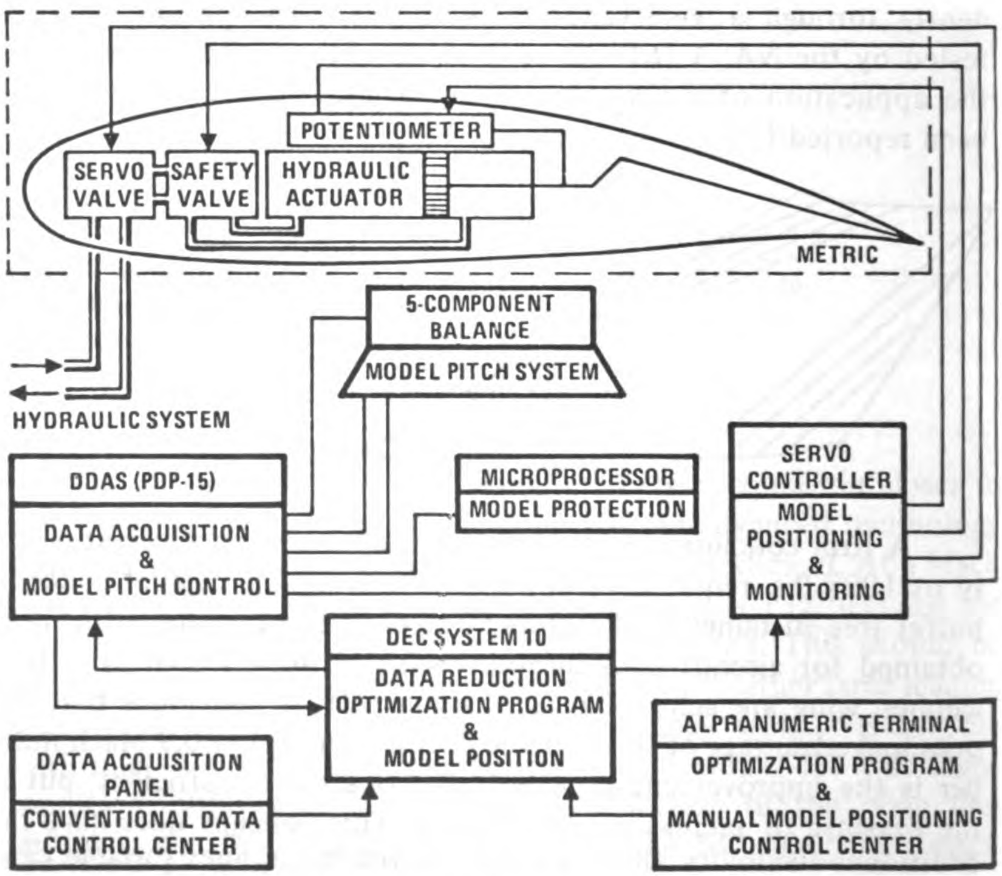

Figure 9 — Soft wing closed-loop testing procedure

Digitized by Google
Original from UNIVERSITY OF MICHIGAN
Generated for member (University of Maryland, College Park) on 2014-10-01 20:21 GMT / http://hdl.handle.net/2027/mdp.39015047405512
Public Domain, Google-digitized / http://www.hathitrust.org/access_use#pd-google

The objective of the concept is to give the designer the ability to automatically optimize wing geometries in the wind tunnel in a shorter time and at less cost than by conventional testing methods. Hopefully, also, the final configuration would be more optimum than that obtained from a finite number of "best guess" configurations. To verify the concept, a two-dimensional self-optimizing model airfoil was designed and built. The model was designed with five variable parameters: conformal leading edge deflection, conformal trailing edge deflection, leading edge radius, lower surface thickness distribution, and lower surface aft camber. The model had a one foot chord and one foot span and was constructed of steel including the flexible leading and trailing edge panels. Internal hydraulic actuators to vary the shape parameters were controlled by a servo system coupled to a digital/analog computer system.

The 2-D model and control system were tested both subsonically and transonically and the results reported [8, 9]. The two-dimensional tests showed that the self-optimization system was stable and convergent.

The first phase of the self optimizing wing investigation showed enough potential that a second phase was undertaken under sponsorship of the Office of Naval Research, the Air Force Flight Dynamics Laboratory, and the Air Force Arnold Engineering Development Center. The purpose of the second phase of the study was to extend the concept to a three-dimensional model wing. This permitted a more realistic assessment of the concept and allowed application of spanwise variations in camber and twist. The three-dimensional wing operates essentially in the same manner as the two-dimensional airfoil. The number of variables in the optimization process of course increases.

A one-sixth scale semi-span model of a modern variable sweep fighter/bomber wing was designed and fabricated (Figure 10). The design included six pairs of internal actuators at each of two spanwise stations. The leading edge had deflection actuators at 15% and 25% chord. The trailing edge had deflection actuators at 65% and 80% chord. In addition there were a pair of leading edge sharpness actuators and a pair of actuators to modify upper surface thickness.

The first test of the model and control system was conducted in August 1977 at Arnold Engineering Development Center in wind tunnel 16T at Mach numbers from 0.6 to 0.95 and the results have been reported in reference 10. The first test verified the convergence and stability of the optimization computer algorithms and the ability of the closed loop computer control system to control the model. Converged optimum solutions were obtained for six of the seven

Generated for member (University of Maryland, College Park) on 2014-10-01 20:21 GMT / http://hdl.handle.net/2027/mdp.39015047405512
Public Domain, Google-digitized / http://www.hathitrust.org/access_use#pd-google
Digitized by Google
Original from
UNIVERSITY OF MICHIGAN

Figure 10 — A one-sixth scale semi-span model of a modern variable sweep fighter/bomber wing.

optimization cases attempted. A typical optimization case for minimum drag is shown in Figure 11. The model experienced reliability problems with the hydraulic actuation system requiring frequent maintenance and repair. In addition, drag levels experienced by the model were significantly higher than comparable data from conventional solid wing models, primarily due to the inability of the model to maintain profile shapes to the required tolerances. Because of these problems, it was difficult to make an accurate evaluation of the feasibility and cost effectiveness of this testing concept. The research is continuing with a redesign of the wing model to correct the deficiencies discussed above and a second wind tunnel test to more accurately evaluate the concept.

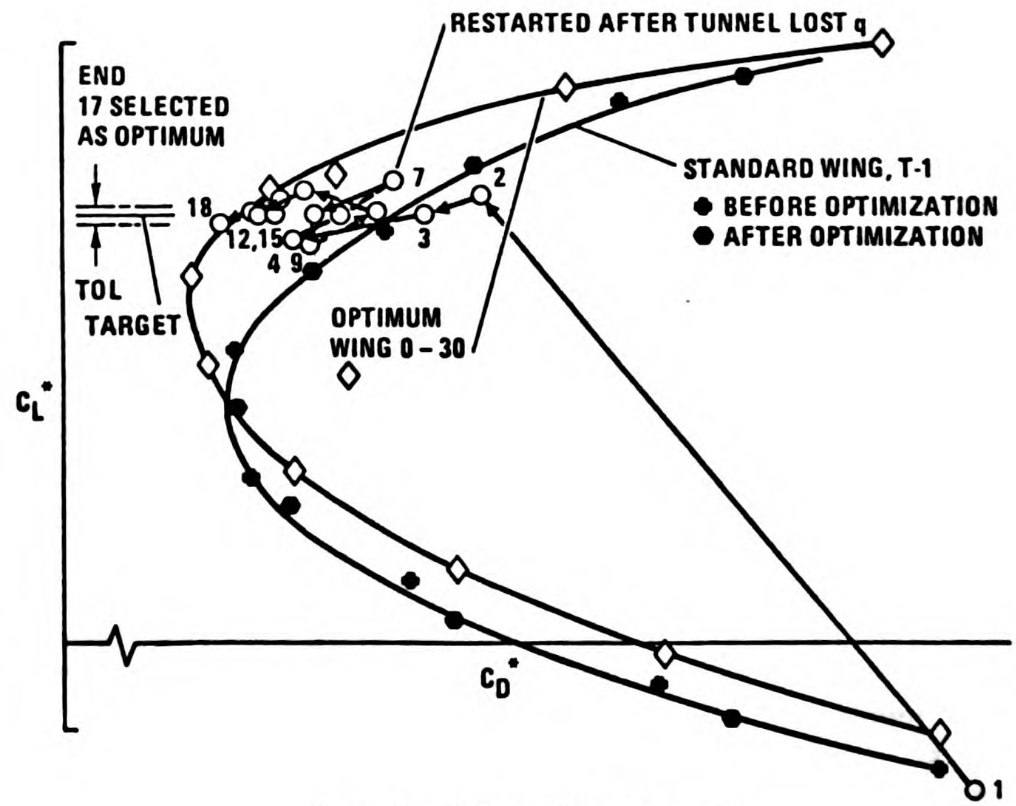

Figure 11 — Soft wing drag minimization

Generated for member (University of Maryland, College Park) on 2014-10-01 20:21 GMT / http://hdl.handle.net/2027/mdp.39015047405512
Public Domain, Google-digitized / http://www.hathitrust.org/access_use#pd-google

Digitized by Google
Original from
UNIVERSITY OF MICHIGAN

Mission Performance Analysis

It is difficult to accurately assess the relative performance improvements of different variable camber concepts that have been developed for different wings and tested under different conditions. To obtain performance data sufficient to make some general observations about the potential of the different concepts, a mission performance analysis program has been used which incorporated the available experimental aerodynamic data for the concepts previously reviewed. Plain leading and trailing edge flaps, conformal leading and trailing edge flaps, leading edge slats, and the segmented leading and trailing edge flaps are considered in the analysis.

A fighter aircraft mission typical of a Navy fleet defense mission was used. One concession made in the fighter mission was to eliminate supersonic dash from the mission profile because of a lack of supersonic data. Since none of the concepts provide significant performance improvements supersonically, this compromise should not affect the relative merits of any concept. The mission includes warm-up, take-off, climb, cruise, loiter, combat, return cruise, landing and reserve segments. The combat mission segment consists of six maximum sustained "g" turns at a mach number of 0.9.

The aircraft design used was typical of current advanced fighter configurations and engines. The aircraft design had a gross take-off weight of 33,830 pounds and a combat thrust-to-weight ratio of 1.05. The basic wing chosen for the analysis was the basic advanced technology wing from reference 5. The aerodynamic data for the conformal and plain flaps were taken from reference 5 and therefore is completely consistant with the basic wing. The data for slats were obtained from references 11 and 12. Trimmed lift and drag increments were obtained and added to the basic wing. For this case the basic wing was used except during the combat phase of the mission; the assumption being that the slats are retractable without a drag penalty at all other times. The segmented flap data was obtained from reference 12. Here also lift and drag increments were obtained after adjusting for scale, trim, and aspect ratio and added to the basic wing.

It is obvious from the survey that each concept offers aerodynamic advantages over the basic fixed camber wing. In application, this improved performance is obtained at a cost of additional complexity and quite possibly additional wing structural weight. The purpose of this performance analysis was to investigate the impact of additional wing structural weight on the mission performance benefits realized from improved aerodynamics. The questions of survivability, maintenance, and reliability are not addressed here.

272-888 O - 78 - 2

Digitized by Google
Original from
UNIVERSITY OF MICHIGAN
Generated for member (University of Maryland, College Park) on 2014-10-01 20:21 GMT / http://hdl.handle.net/2027/mdp.39015047405512
Public Domain, Google-digitized / http://www.hathitrust.org/access_use#pd-google

Initially, the basic wing was run in the mission analysis program. At the same gross weight and fuel load, the plain flap, conformal flap, leading edge slat and segmented flap configurations were used for the same mission using the optimum drag polars for each case. Next the gross weight was held fixed and the assumption was made that increases in wing weight due to the variable camber concepts are accounted for by reducing the fuel load. The mission analysis is re-done for different increments in fuel load for each concept.

Figure 12 shows the change in mission range for each concept for increases in wing weight. The plain flaps, slats, conformal flaps, and segmented flaps have the same range as the basic wing with increases in wing weight of 7.0, 8.5, 17.0 and 30.0 percent respectively. Consequently a 10.0 percent increase in wing weight for the conformal flap reduces its range performance to that of the plain flap. Likewise the segmented flap performance is equivalent to the plain flap with a 23.0 percent increase in wing weight. The rather large increase in range performance of the segmented flap concept is derived primarily from the cruise and loiter segments of the mission.

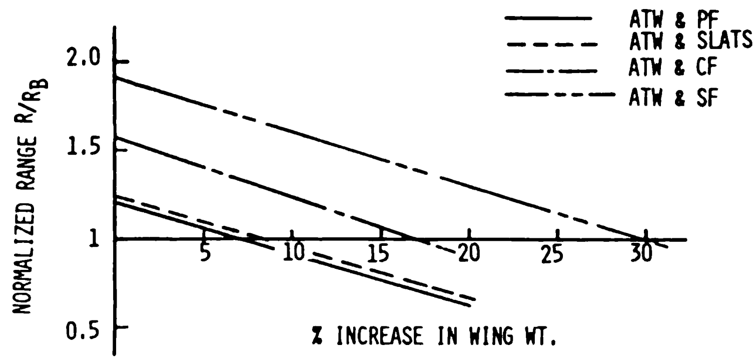

Figure 12 — Range performance vs. wing weight increments

A word of caution should be noted relative to these performance results. The segmented flap data was obtained for a wing with conventional uncambered NACA airfoil sections, see reference 12. This data was incrementally added to the basic advanced technology supercritical wing for the performance analysis. This assumes that similar flap deflections would produce the same drag reductions for the supercritical wing at the low speed loiter conditions. If it does not, this would result in the range for the segmented flap concept being inflated somewhat.

Table 1 lists some of the combat performance parameters for the different concepts. It should be noted that with the type of combat mission chosen, maximum lift coefficient as determined by heavy buffet is not reached by any of the concepts. There are not drastic

Generated for member (University of Maryland, College Park) on 2014-10-01 20:21 GMT / http://hdl.handle.net/2027/mdp.39015047405512
Public Domain, Google-digitized / http://www.hathitrust.org/access_use#pd-google
Digitized by Google
Original from
UNIVERSITY OF MICHIGAN

Table 1
Comparison of Combat Parameters

	ATW & CF	ATW & PF	ATW & SLATS	ATW & SF
Combat Time (T/T_{ATW})	0.878	0.908	0.916	.878
Load Factor ($L.F./L.F._{ATW}$)	1.113	1.097	1.089	1.135
Combat C_L	.7420	.7189	.7146	.7476

differences in maximum lift due to heavy buffet for the different leading edge devices, therefore the relative combat performance should not be significantly different if the combat segment was based on this parameter. The conformal and the segmented flap concepts have essentially the same combat performance and are somewhat better than any of the other concepts.

Conclusions

Based on the foregoing discussion and analysis, the following conclusions are drawn regarding the utilization of variable camber concepts to enhance fighter aircraft "off design" performance.

- Variable camber devices have been successfully employed to improve the transonic maneuvering characteristics of several current fighter airplanes. Those aircraft where variable camber was an "add on" to an existing design did not realize as great a performance improvement as did those aircraft where variable camber was included in the design from the onset.
- Both existing and advanced variable camber concepts yield the greatest improvements in maneuverability in the low to mid Mach number range, i.e., below M = .8, with the performance gains decreasing rapidly at M = .9.
- Most of the data available for conformal variable camber concepts has been obtained for wings with relatively large leading edge radii. For fighter applications, unless the wing sweep is such that the leading edge remains subsonic, this would result in a substantial supersonic drag penalty. Further investigations should be done to demonstrate applicability to thin wings with relatively sharp leading edges.
- Comparative performance analysis of several advanced variable camber concepts has, as would be expected, shown that the

Digitized by Google
Original from
UNIVERSITY OF MICHIGAN
Generated for member (University of Maryland, College Park) on 2014-10-01 20:21 GMT / http://hdl.handle.net/2027/mdp.39015047405512
Public Domain, Google-digitized / http://www.hathitrust.org/access_use#pd-google

choice of a particular concept is very sensitive to the design mission requirements. The "off design" performance due to variable camber can have a major impact on overall mission performance. The segmented flap concept in this study appears to offer the most versatility and allow optimization at more "off design" conditions. The ability to vary the spanwise distribution of camber be very important in advanced concepts.

References

1. Giancomelli, R. and Pistolesi, E., "Historical Sketch", *Aerodynamic Theory*, W.F. Durand, Editor, Pp. 305-394, 1934.
2. Hollingsworth, E.G., and Cohen, M. "Determination of F-4 Aircraft Transonic Buffet Characteristics", *Journal of Aircraft*, Vol. 8 no. 10, October 1971, Pp. 751-763.
3. Buckner, J.K., Hill, P.W., and Benepe, D., "Aerodynamic Design Evaluation of the YF-16," *AIAA Paper 74-935*, presented at AIAA 6th Aircraft Design, Flight Test, and Operation Meeting, Los Angeles, Calif., 12-14 Aug 1974.
4. "F-18 Basic Aerodynamic Data", *McDonnell Aircraft Company Report MDC A3958*, 14 Jan 1976.
5. Gould, Douglas K., "Variable Camber Wing–Phase I–Final Report"; *Boeing Aerospace Co.* Report No. D180-17606-1, October 1973.
6. Ferris, James C.; "Wind Tunnel Investigation of a Variable Camber and Twist Wing", *NASA TN D-8475*, August 1977.
7. Beatty, T.D., Brooks, W.B., and Robinson, L.D., "Investigation of a Variable Camber Wing Design," *Vought Corporation Report*. (NADC-76114-30), to be published.
8. Levinsky, E.S. and Schappelle, R.H.; "Airfoil Optimization Utilizing a Remotely Controlled Flexible Model–Phase I: Low Speed Wind Tunnel Test", *General Dynamics/Convair Division Report No.* CASD-NSC-74-007, August 1974.
9. Levinsky, E.S., Schappelle, R.H. and Pountney, S.; "Airfoil Optimization Through the Adaptive Control of Camber and Thickness–Phase II: Transonic Wind Tunnel Test and Program Summary", *General Dynamics/Convair Division* Report No. CASD-NSC-75-004, September 1975.
10. Levinsky, E.S. and Palko, R.L.; "Semispan Wind Tunnel Test of a Computer-Controlled Self-Optimizing Flexible Technology Wing", *AIAA 10th Aerodynamic Testing Conference Paper 78-786*, April 1978, San Diego, Ca.
11. Lacey, David W.; "Implications on Transonic Maneuverability Based on an Experimental Study of an F-4 Aircraft Model with Quasi-Free Floating Close-Coupled Canard", *DTNSRDC Aviation and Surface Effect Department*, Technical Note AL-303, June 1973.
12. Betkewicz, Peter J., Maj.; "On Airflow Separation and Buffet Onset During Fighter Aircraft Maneuvering", *AGARD Conference Proceedings on Fluid Dynamics of Aircraft Stalling*, AGARD-CP-102, April 1972.

Generated for member (University of Maryland, College Park) on 2014-10-01 20:21 GMT / http://hdl.handle.net/2027/mdp.39015047405512
Public Domain, Google-digitized / http://www.hathitrust.org/access_use#pd-google

Digitized by Google

Original from
UNIVERSITY OF MICHIGAN

On the Heat and Mass Balance of the Arctic Ice Pack

G.A. Maykut*
University of Washington

Introduction

In recent years the increasing strategic and economic importance of the Arctic Basin has stimulated intensified research into the behavior of the ocean-ice-atmosphere system. Sea ice is a key element in this system and is responsible for many of the features which distinguish the Arctic Ocean from other oceans. A quantitative understanding of the way in which the ice influences the exchange of energy between the atmosphere and ocean is of fundamental importance in understanding the overall behavior of the system.

Qualitatively, effects of the ice cover on the atmosphere and ocean appear to be fairly well understood. The high albedo of the ice and its insulation of the atmosphere from the underlying water give rise to a climate over the Arctic Ocean that is more characteristic of continents than of a marine environment. Unlike the ice sheets, however, the ice pack is only a thin veneer (averaging some 3 m in thickness) whose areal extent is sensitive to small changes in heat input from the atmosphere or ocean. Sea ice extent is generally considered to be an important factor in climatic change because it has the potential to amplify small changes in climate through a variety of positive feedback mechanisms (1). For example, a slight cooling of the atmosphere would cause the ice pack to expand, decreasing the amount of solar radiation absorbed at high latitudes; this in turn could result in additional cooling and further expansion of the ice pack. Variations in sea ice extent thus play a central role in many ice age theories (2, 3, 4). Because storm tracks generally tend to follow the margins of the ice pack, changes in ice extent can shift the normal tracks, producing immediate effects on mid-latitude

*Dr. Maykut is Senior Research Associate in The Department of Atmospheric Sciences, University of Washington. For several years he has been conducting research on the sea-air interaction in the arctic for ONR.

Generated for member (University of Maryland, College Park) on 2014-10-01 20:21 GMT / http://hdl.handle.net/2027/mdp.39015047405512
Public Domain, Google-digitized / http://www.hathitrust.org/access_use#pd-google
Digitized by Google
Original from
UNIVERSITY OF MICHIGAN

weather. Such effects appear to be particularly strong in Europe where it has long been noted that unusual weather seems to be correlated with abnormal extent of the ice.

While it has often been assumed that an ice cover suppresses wind mixing in the ocean, the evidence now suggests that moving ice is relatively efficient in transferring momentum from the air to the water. Thermal processes associated with the ice cover thus appear to have the greatest impact on the ocean. In particular, evaporative heat losses and the absorption of solar radiation in the upper ocean are drastically reduced—lack of light beneath the ice is the principal factor limiting biological activity in the Arctic Ocean. The ice also affects vertical motions in the mixed layer; salt rejected by the growing ice forms cold dense brine which sinks, promoting convective overturning. Heat entering the arctic mixed layer is transported upward and rapidly lost to the ice so that, in contrast to the open ocean, no significant storage of heat occurs.

Heat and mass balance measurements have routinely been carried out on most of the U.S. and Soviet drifting stations during the past few decades, producing good data on incident radiation, air and water temperatures, winds, currents, and ocean salinity in many parts of the Arctic Basin (5, 6). Complicating the picture, however, is a strong coupling between dynamic and thermodynamic processes in the ice pack. Strains within the ice create pressure ridges which may reach 20-30 m in thickness, while at the same time producing open leads where there is intense ice growth and rapid heat loss. These relatively small areas of thin ice and open water have the potential to make a large contribution to the overall heat and mass balance of the ice pack. Drifting station measurements, being taken mostly over thick perennial ice, do not include effects of the thin ice and open water; local values derived from such data therefore do not necessarily describe the large-scale processes which ultimately determine how the ice pack interacts with the environment.

It is clear that the total ice production and heat exchange within a particular region can be strongly influenced by variations in ice thickness; however, it is not clear whether there really exist sufficient amounts of thin ice and open water to appreciably alter our present estimates of the monthly and annual totals. We address this question in the following sections, using a combination of theory and observations to examine the magnitude of errors which are likely to be introduced by neglecting thin ice and open water. For many years the Office of Naval Research has supported the author and his colleagues; some of their research results are described here.

Generated for member (University of Maryland, College Park) on 2014-10-01 20:21 GMT / http://hdl.handle.net/2027/mdp.39015047405512
Public Domain, Google-digitized / http://www.hathitrust.org/access_use#pd-google
Digitized by Google
Original from UNIVERSITY OF MICHIGAN

The Ice Thickness Distribution

The ice pack is a mixture of many different thicknesses of ice, ranging from open water to thick pressure ice (Figures 1 and 2). Since many properties of sea ice are strongly dependent upon thickness (e.g. compressive strength, surface temperature, growth rate, etc.), the bulk properties of the ice pack are determined by the way in which thickness varies in time and space. To quantify these thickness variations, we introduce the concept of an *ice thickness distribution*. First let us consider some large region (ten to hundreds of kilometers across) containing many different thicknesses of ice. If we now measure the area covered by ice in selected thickness ranges (e.g. 10-20 cm), we can construct a histogram showing the amount of ice in each thickness category (Figure 3). While the thickness distribution has a more precise mathematical definition (3), we shall use the term here in reference to the histogram.

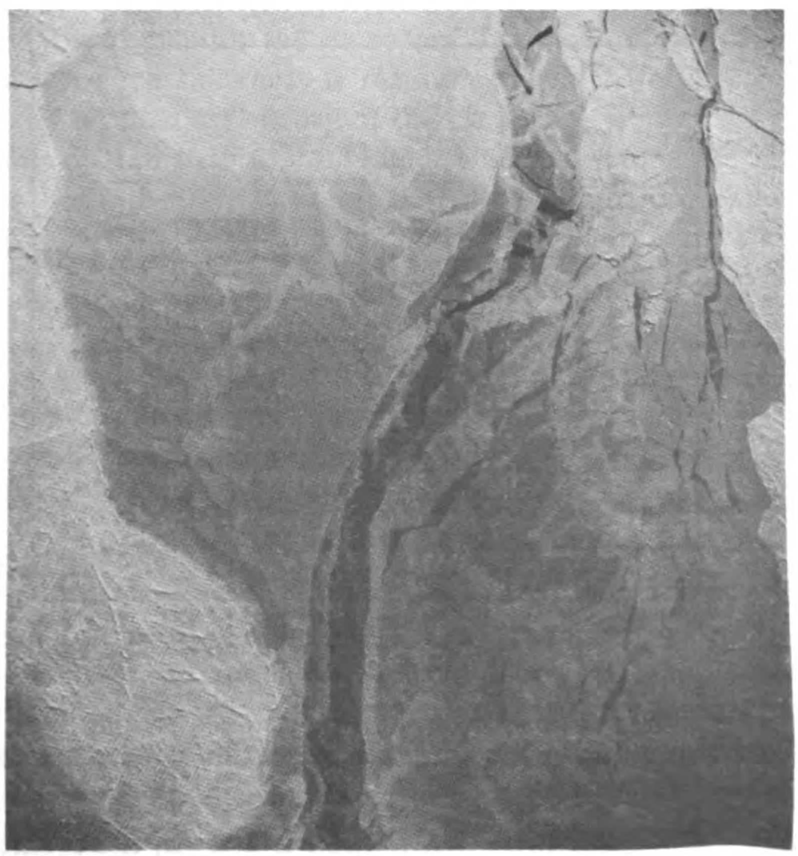

Figure 1 — NAVOCEANO photograph of a region about 15 km across, taken from an altitude of 9 km in April 1972. Ice thickness corresponds approximately to the shade of gray, open water being the darkest. The frame shows a lead that has frozen, partially closed, and opened again. Ice within the lead has rafted in many spots. Pressure ridges in the older ice surrounding the lead are visible in the lower left.

Digitized by Google
Original from UNIVERSITY OF MICHIGAN
Generated for member (University of Maryland, College Park) on 2014-10-01 20:21 GMT / http://hdl.handle.net/2027/mdp.39015047405512
Public Domain, Google-digitized / http://www.hathitrust.org/access_use#pd-google

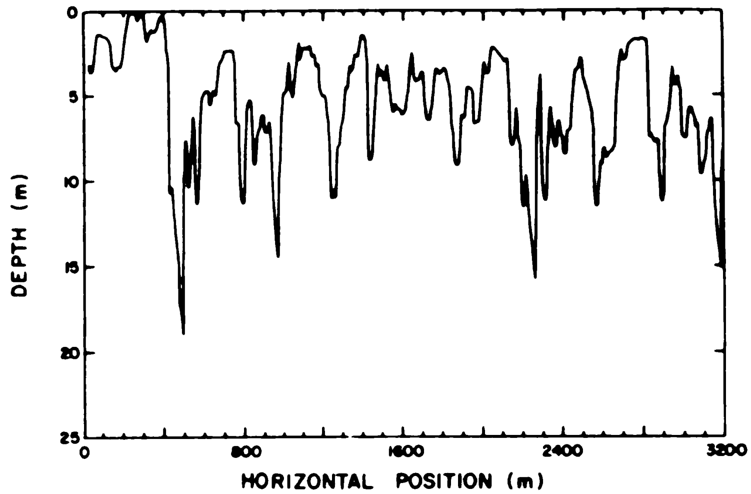

Figure 2 — A profile of the underside of arctic pack ice (after Swithinbank, *1972). The data were acquired from a submarine using upward-looking sonar at about 83°N, 06°E in March 1971.*

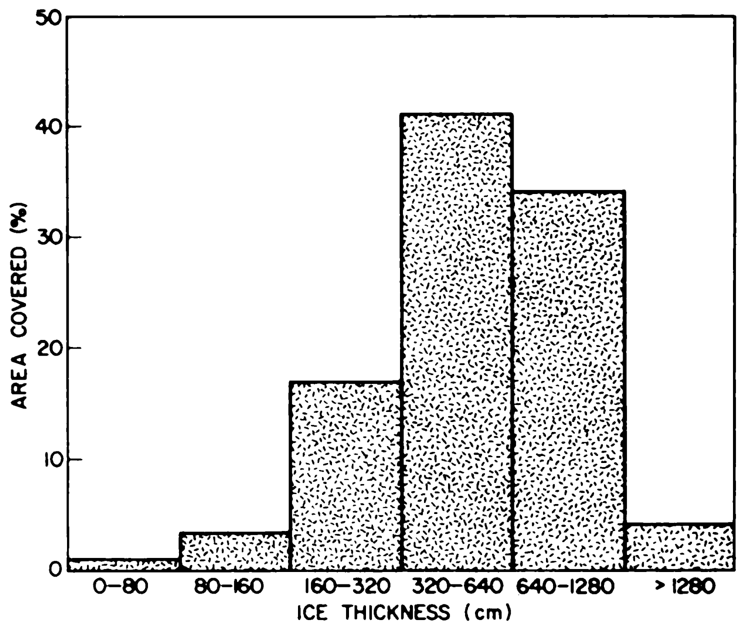

Figure 3 — An observed thickness distribution derived from submarine sonar profiles (LeShack et al., *1971) describing winter ice conditions in the Central Arctic.*

Once the ice thickness distribution is known, it becomes possible to estimate areally-averaged quantities. Unfortunately, the thickness distribution is difficult to determine. Direct measurements can be made from submarine sonar profiles (Figure 3), but such data do not yet adequately resolve the thickness of young ice. An equally serious drawback to the use of submarine data is the lack of informa-

Generated for member (University of Maryland, College Park) on 2014-10-01 20:21 GMT / http://hdl.handle.net/2027/mdp.39015047405512
Public Domain, Google-digitized / http://www.hathitrust.org/access_use#pd-google
Digitized by Google
Original from
UNIVERSITY OF MICHIGAN

tion on temporal variations in the thickness distribution. Young ice, in particular, can undergo large changes in area on time scales of hours to days. An alternate approach is to calculate the thickness distribution theoretically, using more indirect data. To see how this can be done, we need to understand the factors responsible for producing the thickness distribution. The ice pack is in almost constant motion, opening and closing in response to winds and currents. Converging motions tend to crush the thinnest (weakest) ice, piling it into ridges; divergence results in the formation of leads. Ice thickness is also continuously changing in response to thermal processes which cause rapid growth where the ice is thin and slow growth where the ice is thick. On a year-long average, the thermodynamics strives for a single equilibrium thickness (about 3 m in the Central Arctic) by net accretion to the thin ice and net ablation from the thick; by contrast, the dynamics creates regions of thick deformed ice and regions of no ice at all. The thermodynamics thus seek the mean and the dynamics the extremes. Because of this disparity, a distribution of ice thickness is maintained which reflects both the thermal and mechanical history of the ice pack.

A thickness distribution model has been developed (8, 9) which simulates both the dynamic and thermodynamic processes. Input data needed by the model includes seasonally varying growth rates for each ice thickness and large-scale strain rates. The model has been tested in the Central Arctic using a strain history derived from the motions of drifting stations ARLIS II, T-3, and NP-10 during the period 1962-1964; an empirical equation was used to obtain growth rates from measured air temperatures. Results were in reasonable agreement with what little we know about thickness variations in the region. In the thickness distribution calculations reported here, we again make use of strains from the ARLIS II/T-3/NP-10 triangle, but develop a much more realistic treatment of the thermodynamics. Using climatological heat balance data in conjunction with the ice models described in the next section, we were able to calculate growth rates which take into account seasonal changes in incoming solar radiation, snowfall, the dependence of albedo on ice thickness, and variations in the oceanic heat flux. In addition to better growth rates, the improved thermodynamics also provided the basis for regional estimates of the heat and mass balance.

Energy Exchange Over Young Sea Ice

During the winter the rates of turbulent heat exchange, ice growth, and salt rejection depend strongly on ice thickness being up to two orders of magnitude larger over a refreezing lead than over

Digitized by Google
Original from
UNIVERSITY OF MICHIGAN
Generated for member (University of Maryland, College Park) on 2014-10-01 20:21 GMT / http://hdl.handle.net/2027/mdp.39015047405512
Public Domain, Google-digitized / http://www.hathitrust.org/access_use#pd-google

perennial ice (10, 11). Although decreasing rapidly with increasing ice thickness (see Figure 4), these rates can still be an order of magnitude larger over 40-50 cm ice than over 3 m ice. Somewhat less sensitive to ice thickness than the quantities mentioned above are absorbed short-wave radiation and emitted long-wave radiation. During the summer there is little thermal distinction between ice of different thicknesses, but leads admit large amounts of short-wave radiation to the ocean which must ultimately affect the mass balance of the ice pack.

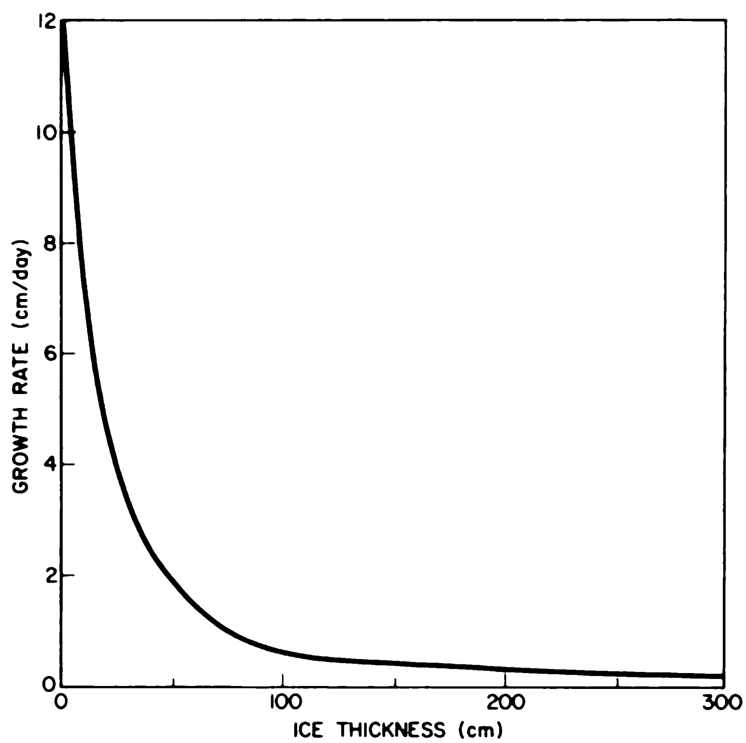

Figure 4 — Dependence of mid-winter growth rates in the Central Arctic on ice thickness.

To determine how thickness variations influence the regional heat and mass balance, we must know explicitly how each of the fluxes changes with thickness and season. Since it is obviously impractical to carry out measurements over every thickness of ice, we use theoretical models which allow us to extrapolate data obtained over thick ice to ice of any thickness. Separate models were developed for young (< 80 cm) ice and thick ice. Both models employ heat balance equations to describe mass and temperature changes at the top and bottom of the ice. The basic idea is that a boundary receiving more energy than it loses will, depending on its tempera-

Generated for member (University of Maryland, College Park) on 2014-10-01 20:21 GMT / http://hdl.handle.net/2027/mdp.39015047405512
Public Domain, Google-digitized / http://www.hathitrust.org/access_use#pd-google
Digitized by Google
Original from
UNIVERSITY OF MICHIGAN

ture, either become warmer or melt; similarly, an energy deficit results in either cooling or ice growth. The situation at the lower boundary is relatively simple, there being only an oceanic heat flux and a conductive heat flux in the ice to consider. Since the temperature at the bottom of the ice must remain at the freezing point of the ocean, only ablation or accretion may occur. At the upper surface, however, there are many more ways to exchange energy. Fluxes considered in the models thus must include: incoming, transmitted, and reflected shortwave radiation, incoming and emitted longwave radiation, sensible heat, latent (evaporation and condensation) heat, and heat conducted through the ice.

Despite similarities in overall form, the two models are different in several respects. Temperature profiles in young ice are nearly linear so that growth rates depend directly on the surface temperature. Thicker ice, however, has a more complex temperature structure, and growth rates depend more on the thermal history of the ice than on immediate surface conditions. For example, as the ice warms slowly downward in the early summer, it is possible for thick ice to be melting at the surface while continuing to grow at the bottom. The thick ice model therefore requires an additional equation to describe the storage and transport of heat within the ice. This model and its applications have been described previously in *Naval Research Reviews* (12). While we are able to assume that the turbulent heat fluxes are independent of ice thickness in the thick ice model, this does not hold for young ice. The fluxes of sensible and latent heat depend on the temperature gradient in the atmospheric boundary layer which can undergo large changes in magnitude during the early stages of ice growth. To take such changes into account the upper boundary condition of the young ice model was reformulated so that the specified turbulent heat fluxes could be replaced by air temperature and wind speed data. Sensible heat flux variations predicted by this model are illustrated in Figure 5. Another difference between the two models is in the treatment of the oceanic heat flux. Large amounts of shortwave radiation can pass through thin ice, augmenting the upward flux of heat from the deeper ocean. This effect must be taken into account in the young ice model, but can be neglected in the thick ice where shortwave transmission is small.

To operate these models we must specify the amount of incoming longwave and shortwave radiation, air temperature, wind speed, relative humidity, snowfall, and upward heat flux to the mixed layer. Built into the models are data on the thermal and

Digitized by Google
Original from
UNIVERSITY OF MICHIGAN
Generated for member (University of Maryland, College Park) on 2014-10-01 20:21 GMT / http://hdl.handle.net/2027/mdp.39015047405512
Public Domain, Google-digitized / http://www.hathitrust.org/access_use#pd-google

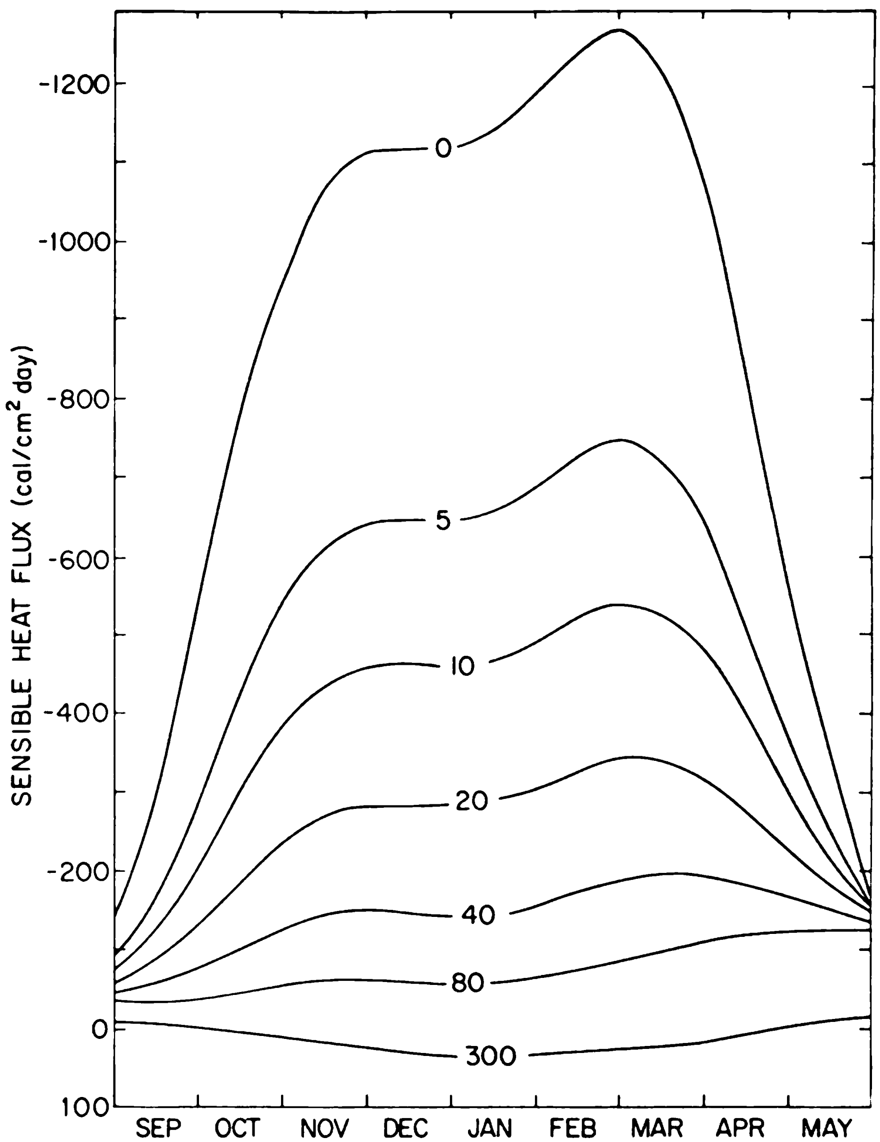

Figure 5 — Seasonal variations in the sensible heat flux over various thicknesses (em) of ice as predicted by the young ice model.

optical properties of the ice, as well as assumed salinity profiles in the ice. With this information the models then predict mass changes, temperatures, and all other heat fluxes as a function of ice thickness. Since brine rejection is related to growth rates (13), the salt flux to the mixed layer can also be determined.

Regional Heat and Mass Balance

We now have the tools needed to estimate large-scale fluxes. As an example let us consider the regional ice production. From the thickness distribution model we can calculate the fractional area

Generated for member (University of Maryland, College Park) on 2014-10-01 20:21 GMT / http://hdl.handle.net/2027/mdp.39015047405512
Public Domain, Google-digitized / http://www.hathitrust.org/access_use#pd-google
Digitized by Google
Original from UNIVERSITY OF MICHIGAN

covered by each thickness category, and from the thermodynamic models we can calculate growth rates in each category. The contribution made by a particular thickness category to the total ice production is found by simply multiplying its fractional area by its rate of ice growth. Repeating this procedure for each thickness category and then summing up the individual contributions gives the average rate of ice production within the region for which the thickness distribution is defined. Regional heat fluxes are determined in the same way. Thermodynamic input data for the models (see Table 1) were taken from climatological averages in the Central Arctic (5). Heat input from the deeper ocean was assumed to be 125 cal/(cm^2 month) and the wind speed to average 5 m/sec. Strain data came from the ARLIS II/T-3/NP-10 triangle. Thickness categories were chosen to provide fine resolution where the heat fluxes change rapidly with thickness, and more coarse resolution where the fluxes are less sensitive to thickness. On this basis, eight categories were selected: 0-10, 10-20, 20-40, 40-80, 80-160, 160-320, 320-640, and ice thicker than 640 cm. Although thickness distributions and regional fluxes were calculated at 6 hour intervals for the entire period from May 1962 to May 1964, the discussions here will focus on results from 1963.

Table 1
Monthly Totals and Averages for Quantities Used as Input to the Thermodynamic Calculations

	JAN	FEB	MAR	APR	MAY	JUN	JUL	AUG	SEPT	OCT	NOV	DEC
Incoming Shortwave Radiation (kcal/cm^2 month)	0	0	2.4	10.0	17.4	18.7	13.7	8.8	3.7	0.5	0	0
Incoming Longwave Radiation (kcal/cm^2 month)	10.4	10.3	10.3	11.8	15.1	17.9	19.1	18.6	16.5	13.8	11.4	10.8
Air Temperature at 10 m (°C)	-29.4	-32.0	-31.2	-22.7	-10.5	-1.2	-0.6	-1.4	-9.9	-19.8	-27.8	-29.2
Relative Humidity	0.85	0.85	0.88	0.88	0.89	0.93	0.93	0.94	0.88	0.85	0.85	0.85

Monthly and annual averages for each category in the thickness distribution are shown at the top of Table 2. The amount of ice in the thinnest category (0-10 cm) averaged 0.2-0.4% during the winter and spring, essentially reflecting strains occurring during the preceeding day. The amount of young (< 80 cm) ice varied from 4-6% during the same period. Satellite data (14) suggest that the amount

Digitized by Google
Original from UNIVERSITY OF MICHIGAN
Generated for member (University of Maryland, College Park) on 2014-10-01 20:21 GMT / http://hdl.handle.net/2027/mdp.39015047405512
Public Domain, Google-digitized / http://www.hathitrust.org/access_use#pd-google

Generated for member (University of Maryland, College Park) on 2014-10-01 20:21 GMT / http://hdl.handle.net/2027/mdp.39015047405512
Public Domain, Google-digitized / http://www.hathitrust.org/access_use#pd-google

Digitized by Google

TABLE 2

THICKNESS DISTRIBUTION AVERAGES AND AREA-WEIGHTED FLUXES FOR 1963. REGIONAL FLUX TOTALS ARE COMPARED WITH THOSE CORRESPONDING TO A UNIFORM 3 M ICE COVER

		JAN	FEB	MAR	APL	MAY	JUN	JUL	AUG	SEP	OCT	NOV	DEC	ANNUAL
Average area covered by ice in each thickness category (%)	0-10	0.3	0.3	0.2	0.6	1.7	3.3	7.7	12.6	3.6	0.8	0.3	0.4	2.7
	10-20	0.5	0.5	0.4	0.8	1.0	0.2	0.3	0.8	3.6	1.4	0.6	0.7	0.9
	20-40	1.5	1.3	0.9	1.5	1.2	0.3	0.9	1.7	5.6	3.7	1.4	1.6	1.8
	40-80	6.0	3.7	2.4	2.3	2.3	0.7	2.7	3.7	6.9	13.6	12.1	7.6	5.3
	80-160	11.5	13.8	14.6	14.0	14.2	14.1	14.2	14.2	15.3	19.8	26.8	29.9	16.9
	160-320	43.3	43.0	42.9	41.7	40.3	40.6	35.7	31.4	30.2	28.2	28.7	31.2	36.4
	320-640	23.3	24.0	25.8	26.9	27.5	29.0	27.1	24.9	24.4	22.6	21.0	20.1	24.7
	640-∞	13.6	13.4	12.8	12.2	11.8	11.8	11.4	10.7	10.4	9.9	9.1	8.5	11.3
Conductive heat flux (cal/cm^2 month)	0-10	72	78	49	106	90	65	139	152	184	135	81	109	1260
	10-20	78	84	57	82	47	0	0	2	117	132	83	106	788
	20-40	139	128	88	91	37	0	0	2	147	220	122	148	1122
	40-80	320	213	133	81	32	0	0	2	111	465	593	396	2346
	80-∞	714	758	522	55	-514	-3	0	163	512	697	775	711	4390
	TOTAL	1323	1261	849	415	-308	62	139	321	1071	1649	1654	1470	9906
	3 m	778	804	543	56	-545	-96	0	63	633	867	905	792	4800
Sensible heat flux (cal/cm^2 month)	0-10	-50	-56	-36	-75	-75	-23	-25	-63	-110	-88	-56	-76	-733
	10-20	-53	-59	-42	-63	-44	-2	-1	-4	-74	-85	-57	-73	-557
	20-40	-85	-85	-63	-79	-47	-3	-3	-8	-95	-135	-78	-94	-775
	40-80	-153	-120	-88	-87	-81	-9	-9	-18	-77	-247	-315	-206	-1410
	80-∞	1017	760	659	239	-363	-376	-287	-304	-136	102	469	746	2526
	TOTAL	676	440	430	-65	-610	-413	-325	-397	-492	-453	-37	297	-949
	3 m	1110	806	686	250	-385	-393	-325	-374	-171	128	545	831	2708

Original from UNIVERSITY OF MICHIGAN

Generated for member (University of Maryland, College Park) on 2014-10-01 20:21 GMT / http://hdl.handle.net/2027/mdp.39015047405512
Public Domain, Google-digitized / http://www.hathitrust.org/access_use#pd-google

Digitized by Google

Latent heat flux (cal/cm^2 month)	0-10	-7	-7	-5	-17	-38	-29	-50	-88	-64	-23	-9	-11	-348
	10-20	-6	-5	-4	-12	-17	-2	-2	-5	-44	-20	-7	-8	-132
	20-40	-8	-7	-5	-15	-18	-3	-6	-12	-52	-32	-9	-9	-176
	40-80	-15	-9	-7	-16	-35	-9	-17	-26	-47	-66	-38	-21	-306
	80-∞	0	0	0	-86	-432	-652	-581	-516	-315	-147	0	0	-2729
	TOTAL	-36	-28	-21	-146	-540	-695	-656	-647	-522	-288	-63	-49	-3691
	3 m	0	0	0	-92	-460	-682	-656	-634	-393	-182	0	0	-3099
Rate of ice production (cm/cm^2 month)	0-10	1.1	1.2	0.7	1.5	0.6	-0.4	0	-0.7	2.4	2.1	1.2	1.7	11.4
	10-20	1.2	1.3	0.9	1.1	0.4	-0.1	-0.2	-0.2	1.5	2.0	1.3	1.6	10.8
	20-40	2.1	2.0	1.3	1.2	0.3	-0.1	-0.5	-0.4	1.9	3.3	1.9	2.2	15.2
	40-80	4.8	3.2	2.0	1.0	0.2	-0.3	-1.5	-0.8	1.4	6.8	8.9	6.0	31.7
	80-160	1.6	2.4	2.6	1.4	0.7	-0.7	-4.9	-1.7	-0.2	1.6	3.6	3.7	10.1
	160-320	3.6	3.8	3.9	3.3	2.0	-1.2	-11.5	-3.1	-0.7	-0.4	1.1	2.3	3.1
	320-640	0.3	0.6	0.8	0.9	0.9	0.7	-6.1	-2.0	-0.2	-0.2	-0.2	-0.1	-4.6
	640-∞	-0.2	-0.2	-0.2	-0.2	-0.2	-0.2	-2.9	-1.1	-0.2	-0.2	-0.2	-0.2	-6.0
	TOTAL	14.5	14.3	12.0	10.2	4.9	-2.3	-27.6	-10.0	5.9	15.0	17.6	17.2	71.7
	3 m	7.3	7.4	7.7	7.1	5.1	2.0	-30.9	-9.1	-1.8	-1.7	0.8	6.1	0.0
Short-wave radiation absorbed below 3 m in the ocean (cal/cm^2 month)	0-10			1	20	101	248	457	414	58	2			1301
	10-20			2	21	40	9	11	17	41	2			143
	20-40			4	29	36	9	21	27	36	4			166
	40-80			6	25	41	13	37	34	23	7			186
	80-∞			0	0	0	0	67	42	0	0			109
	TOTAL			13	95	218	279	593	534	158	15			1905
	3 m			0	0	0	0	57	41	0	0			98
Salt flux (gm/cm^2 month)$\cdot 10^3$	0-10	15	15	10	24	14	0	0	8	47	34	17	23	207
	10-20	21	22	15	21	9	0	0	0	31	37	22	28	206
	20-40	40	37	25	23	7	0	0	0	41	65	35	42	315
	40-80	96	64	39	22	5	0	0	0	31	142	179	119	697
	80-∞	231	265	287	265	193	97	3	0	1	29	118	183	1672
	TOTAL	403	403	376	355	228	97	3	8	151	307	371	395	3097
	3 m	157	177	184	171	126	52	0	0	0	0	25	122	1014

Original from UNIVERSITY OF MICHIGAN

of young ice is highly variable. During March 1973, for example, it was found that at least 15% of the Beaufort Sea was covered by young ice, but in March 1974 this value was only 6%. Submarine data (15) indicate that young ice comprises 8-12% of the ice pack between January and May. The maximum thickness of young ice included in these estimates is not known, but seems unlikely to exceed 80 cm. The evidence thus suggests that our young ice estimates for the winter and spring may be somewhat conservative. The greatest amount of open water was found to occur in August when it averaged about 12%. An aerial mosaic made over the Beaufort Sea in mid-August 1975 (Figure 6) shows that open water accounted for about 11% of the area, in excellent agreement with out theoretical values. In light of our present knowledge, the thickness distributions used to estimate the regional fluxes appear to be quite reasonable.

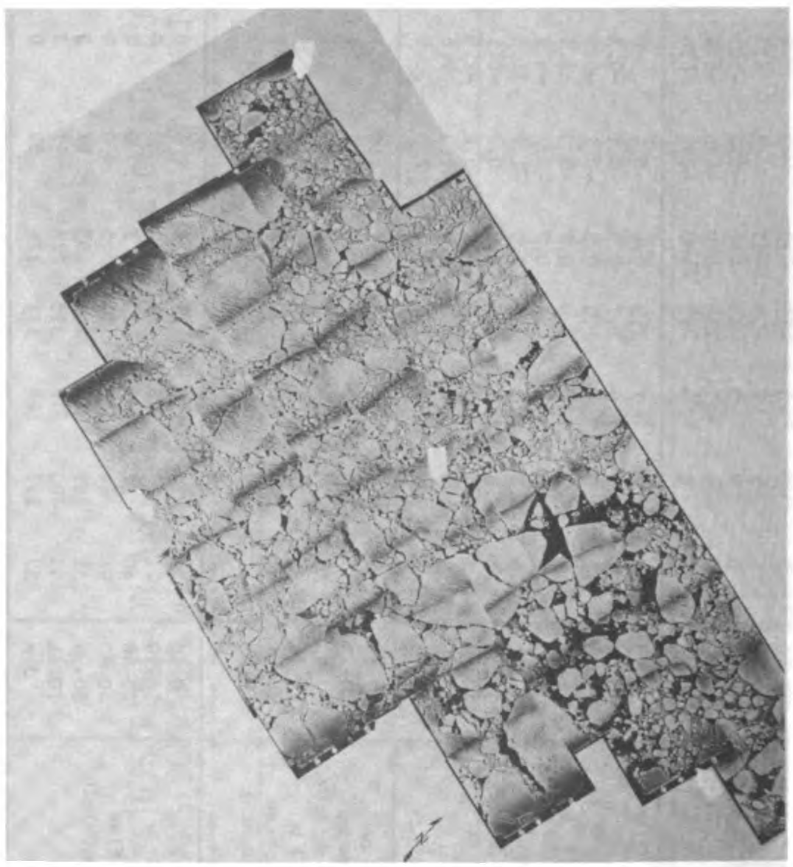

Figure 6 — Aerial mosaic of a portion of the Beaufort Sea (centered on 75°N, 140°W) assembed from NASA photographs taken on 18 August 1975 from an altitude of 11 km. The picture spans an area roughly 100 by 200 km in size. About 11% of the area is open water. White arrows denote positions of the 4 manned camps in the Arctic Ice Dynamics Joint Experiment (AIDJEX) strain array.

Digitized by Google
Original from
UNIVERSITY OF MICHIGAN
Generated for member (University of Maryland, College Park) on 2014-10-01 20:21 GMT / http://hdl.handle.net/2027/mdp.39015047405512
Public Domain, Google-digitized / http://www.hathitrust.org/access_use#pd-google

Regional heat and mass fluxes were also determined at 6 hour intervals and then integrated over time to produce the monthly and annual values shown in Table 2. The radiation fluxes were found to be only mildly affected by the thickness distribution–net shortwave radiation increased by 5-8% during the summer, while the net longwave radiation loss was typically 3-4% larger during the cold months. Ice production, on the other hand, was dramatically larger. Figure 7(a) shows the net annual ice production in each of the thickness categories, averaged over the area of the triangle. The mass of ice produced in the 0-10 cm category, for example, was equivalent to a layer 11.4 cm in thickness covering the entire triangle. Annual net ice production for the region was found to be 71.7 cm/cm^2, in contrast to the zero mass balance which would have been obtained if the ice pack were assumed to be a uniform 3 m cover. Ice thicker than 3 m experienced a net mass loss, while growth in areas of young ice accounted for nearly all the ice production. Despite the extremely large growth rates in newly-formed leads, ice production in the 0-10 cm category was only about 35% as large as that in the 40-80 cm category. This simply reflects the greater area covered by ice in the 40-80 cm range. Seasonal variations in the regional ice production are shown in Figure 7(b). Although the regional ice production during the winter was about twice as large as the 3 m values, the largest differences occurred during the fall. In the thick ice heat stored during the summer retarded fall heat losses at the bottom, allowing a small amount of ablation to take place; however, fall ice growth in the large areas of open water formed during the summer was rapid, accounting for the net ice production within the region. Seasonal variations in the salt flux paralleled the ice production, but the total amount of salt added to the mixed layer during the freezing season was about three times that expected from a thick uniform cover.

The amount of heat conducted through the ice to the surface increased from 4.8 to 9.9 kcal/(cm^2 year) when the contributions from young ice were taken into account. Most of this additional heat was lost via the turbulent heat fluxes. Figure 8(a) shows the annual turbulent heat losses over each of the young ice categories. Because the turbulent fluxes depend weakly on thickness once the ice exceeds 80 cm, the thicker ice is shown as a single category. While all categories sustained a net turbulent heat loss for the year, ice in the 20-80 cm range provided over half the regional total. The magnitude of the turbulent heat exchange is directly related to the rate of ice growth, and as Figure 8(b) shows, the greatest differences between regional and 3-m values occurred during the fall when regional ice

Digitized by Google
Original from
UNIVERSITY OF MICHIGAN
Generated for member (University of Maryland, College Park) on 2014-10-01 20:21 GMT / http://hdl.handle.net/2027/mdp.39015047405512
Public Domain, Google-digitized / http://www.hathitrust.org/access_use#pd-google

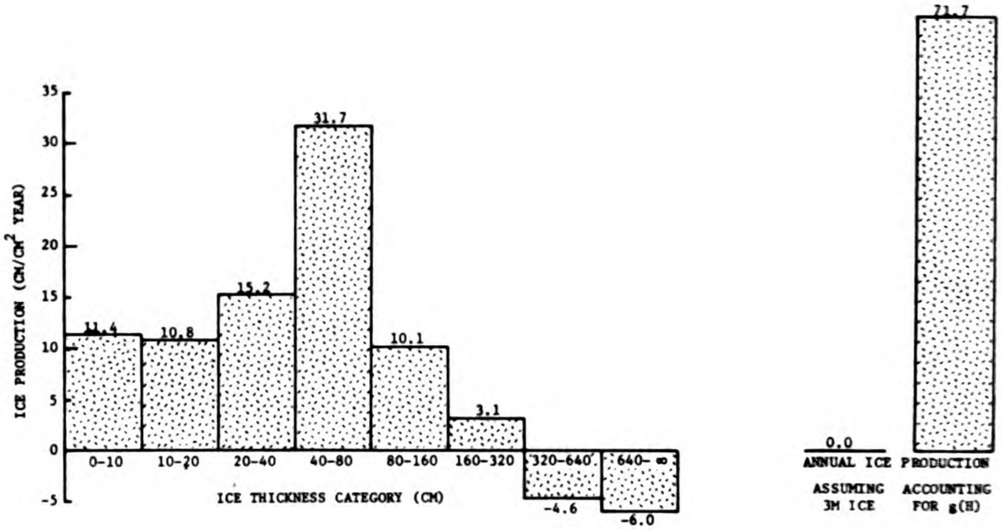

(a)

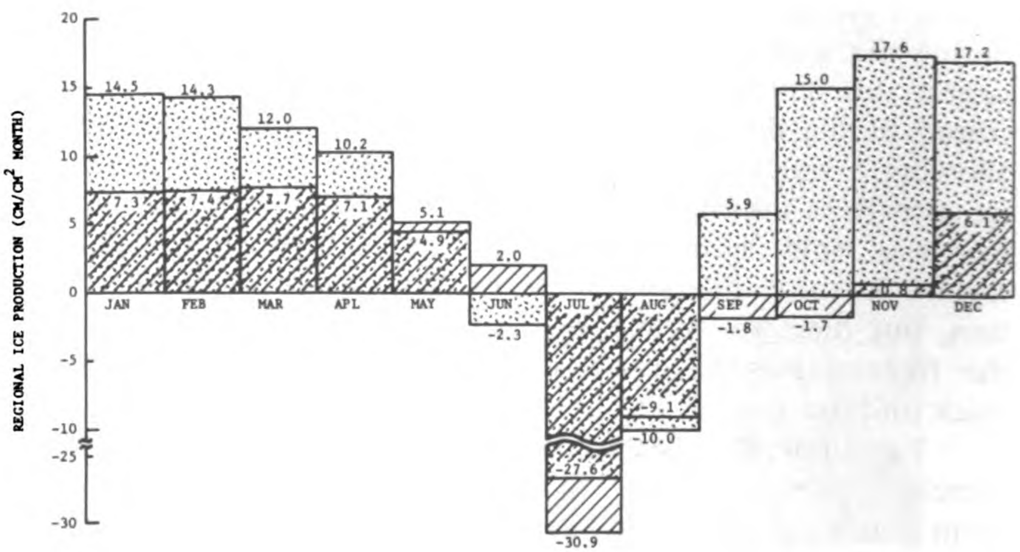

(b)

Figure 7 — Ice production during 1963. (a) Annual totals in each thickness category. (b) Monthly totals obtained by taking account the thickness distribution g(H), [stippled] and by assuming a uniform 3 m cover [cross-hatched.]

Digitized by Google
Original from UNIVERSITY OF MICHIGAN
Generated for member (University of Maryland, College Park) on 2014-10-01 20:21 GMT / http://hdl.handle.net/2027/mdp.39015047405512
Public Domain, Google-digitized / http://www.hathitrust.org/access_use#pd-google

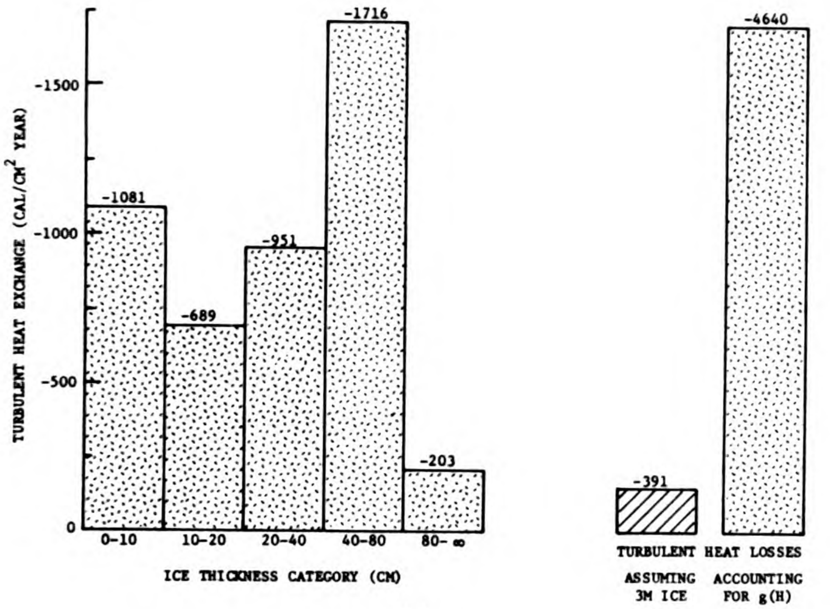

(a)

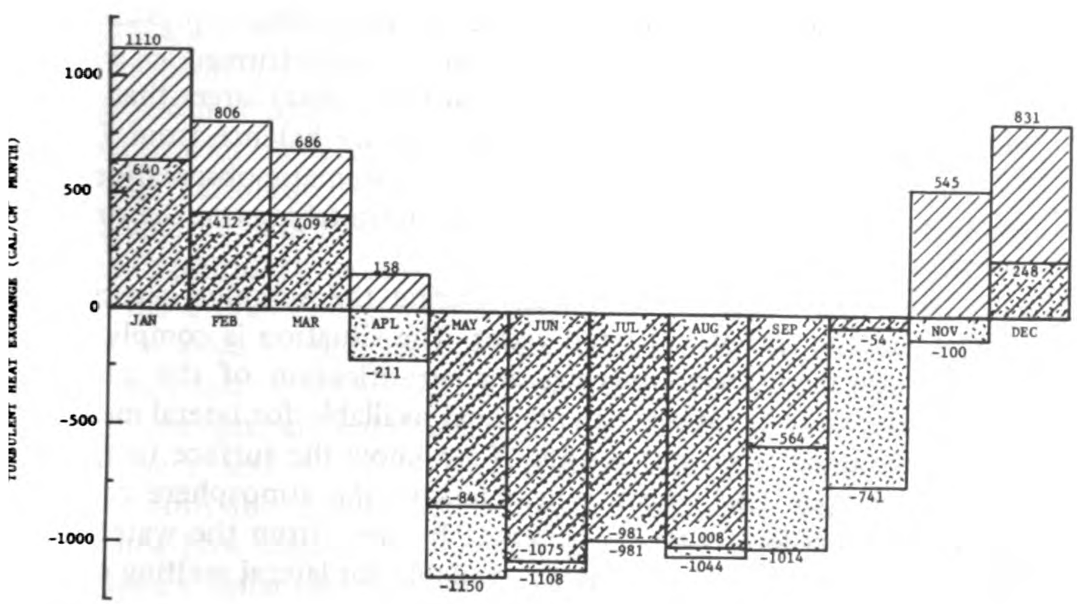

(b)

Figure 8 — Total turbulent heat exchange during 1963. (a) Annual totals in each thickness category. (b) Monthly totals obtained by taking into account the thickness distribution, g(H), [stippled] and by assuming a uniform 3 m ice cover [cross-hatched].

Generated for member (University of Maryland, College Park) on 2014-10-01 20:21 GMT / http://hdl.handle.net/2027/mdp.39015047405512
Public Domain, Google-digitized / http://www.hathitrust.org/access_use#pd-google
Digitized by Google
Original from
UNIVERSITY OF MICHIGAN

production was large. Periods of strong divergence during the winter resulted in negative regional totals for a few days at a time, but monthly totals remained positive between December and April.

During the summer substantial amounts of solar radiation enter the ocean through leads, causing a decrease in the ice concentration and a general thinning of the remaining ice. To study this problem we assumed: (i) that shortwave radiation absorbed between the surface of the lead and the bottom of the surrounding ice would be lost by lateral melting on the lead walls and by heat exchange with the atmosphere, and (ii) that radiation absorbed below the 3 m level in the ocean would be advected beneath the ice. We found that approximately 1.9 kcal/(cm^2 year) was absorbed beneath the ice pack. This is about 20 times larger than the amount transmitted by 3 m ice and is somewhat larger than present estimates of the heat reaching the ice from the Atlantic layer (1.5 kcal/cm^2 year). Although a large fraction of this energy must go into melting on the bottom of the ice, it is still not clear how this affects the overall mass balance of the pack. Theoretical calculations (12) show that, if the ice pack were horizontally uniform, an oceanic heat flux of 3.4 kcal/(cm^2 year) would result in average ice thicknesses roughly one-half present day values. We suspect that much of the additional heat supplied to the mixed layer by shortwave radiation is utilized in the melting of pressure ice eroded from ridge keels. If this is the case, then deformed ice would have to sustain a mass loss about 25 cm/(cm^2 year) larger than that indicated in Table 2, dropping the regional ice balance from 72 to 47 cm/(cm^2 year). Until we can carry out systematic observations of decay rates in deformed ice, we cannot definitely settle the uncertainties in the regional mass balance.

Lateral melting on lead walls during the summer causes an increase in the amount of open water. The situation is complicated by ice movement, wind mixing, and stratification of the surface waters, but a crude estimate of the heat available for lateral melting can be obtained from our results. If we know the surface temperature of an open lead, the net heat loss to the atmosphere can be calculated; this loss must be balanced by heat from the water. We therefore assumed that the energy available for lateral melting could be approximated by the difference between the shortwave radiation absorbed in the upper 3 m of the ocean and the net heat loss at the surface. With a surface temperature of 0°C, we found that about 600 cal/(cm^2 year) were potentially available for lateral melting. This is sufficient to add about 3% to the amount of open water created by vertical melting and dynamic processes.

Generated for member (University of Maryland, College Park) on 2014-10-01 20:21 GMT / http://hdl.handle.net/2027/mdp.39015047405512
Public Domain, Google-digitized / http://www.hathitrust.org/access_use#pd-google
Digitized by Google
Original from UNIVERSITY OF MICHIGAN

Discussion

The regional values reported above should not necessarily be taken to be representative of average conditions in the Central Arctic. Year-to-year variations are expected to be large and typical strain conditions are not yet known. For example, there was strong convergence in the ice pack during October 1962, causing the area of the triangle to decrease by 16%; during the same period in 1963 the area of the triangle increased by 12%. Likewise, satellite data (14) taken over the same region indicated that the area covered by young ice differed by at least 10% in March 1973 and March 1974. Such large differences in the amount of thin ice should be reflected in the regional fluxes. It is likely that strain histories can be quite different in different parts of the Arctic Basin (e.g. Beaufort Gyre and Transpolar Drift Stream), so that the regional fluxes may also exhibit large spatial variations. Further analysis of existing data and results from future buoy programs should provide the information needed to address these problems.

Although the results obtained here must be treated as preliminary, we believe that they provide a general picture of how thin ice and open water influence the heat and mass balance of the ice pack. The calculations show that intermediate thickness (20-80 cm) of young ice contribute at least as much to the regional ice production and turbulent heat exchange as do open water and thick ice. Models which consider only thick ice or thick ice and open water therefore cannot provide an accurate determination of these fluxes.

The calculations suggest that the interaction between atmosphere and ocean in the presence of a dynamic ice cover is more vigorous than previously believed. At this point, however, it is difficult to assess the overall impact on the region. The large amount of ice produced in areas of thin ice goes partly into building pressure ridges and partly into replacing ice exported from the region, but the relative proportions are unknown. The large turbulent heat input to the atmosphere and salt flux to the ocean should create convective plumes both above and below refreezing leads, but again we do not yet know how these affect the large-scale characteristics of the boundary layers. Solar energy absorbed in leads is clearly important to the mass balance of the ice pack; in particular, it is likely to be one of the principal factors determining the rate at which the ice retreats during the summer. Nevertheless, we need to know a great deal more about the details of this process before we can incorporate it into realistic ice extent and mass balance models. Counterbalancing our lack of knowledge in these areas has been the dramatic increase in

Generated for member (University of Maryland, College Park) on 2014-10-01 20:21 GMT / http://hdl.handle.net/2027/mdp.39015047405512
Public Domain, Google-digitized / http://www.hathitrust.org/access_use#pd-google
Digitized by Google
Original from
UNIVERSITY OF MICHIGAN

imaging and remote data-taking capabilities made possible by recent satellites. While the availability of high quality remote sensing data has provided us with the opportunity to view the Arctic Basin as a whole, interpretation of such data has been limited by an incomplete understanding of certain small-scale processes. The work described above has served to identify several areas where careful theoretical and experimental studies can contribute to this understanding, and hence to more complete utilization of future satellite and buoy data.

References

1. W.W. Kellogg, "Climatic feedback mechanisms involving the polar regions". *In* (G. Weller and S.A. Bowling, eds.) *Climate of the Arctic*, p. 111-116, Geophysical Institute, University of Alaska, 1975.
2. C.E.P. Brooks, *Climate Through the Ages,* 395 pp., McGraw-Hill, New York, 1949.
3. M. Ewing and W.L. Donn, "A theory of ice ages". *Science*, **123**, 1061-1066, 1956.
4. M.I. Budyko, "Polar ice and climate". *In* (J.O. Fletcher, ed.) *Proceedings of the Symposium on the Arctic Heat Budget and Atmospheric Circulation*, p. 3-22, The RAND Corporation, RM-5233-NSF, 1966.
5. J.O. Fletcher, *The Heat Budget of the Arctic Basin and Its Relation to Climate*, 179 pp., The RAND Corporation, R-444-PR, 1965.
6. K. Aagaard and P. Greisman, "Toward new mass and heat budgets for the Arctic Ocean". *J. Geophysical Research*, **80**, 3821-3827, 1975.
7. C. Swithinbank, "Arctic pack ice from below." *In* (T. Karlsson, ed.) *Sea Ice: Proceedings of an International Conference*, p. 246-254, National Research Council, Reykjavik, 1972.
8. A.S. Thorndike and G.A. Maykut, "On the thickness distribution of sea ice." *AIDJEX Bulletin*, **21**, 31-48, 1973.
9. A.S. Thorndike, D.A. Rothrock, G.A. Maykut, and R. Colony, "The thickness distribution of sea ice." *J. Geophysical Research*, **80**, 4501-4513, 1975.
10. F.I. Badgley, "Heat balance at the surface of the Arctic Ocean" *In* (J.O. Fletcher, ed.) *Proceedings of the Symposium on the Arctic Heat Budget and Atmospheric Circulation*, p. 267-278, The RAND Corporation, RM-5233-NSF, 1966.
11. G.A. Maykut, "Energy exchange over young sea ice in the Central Arctic." *J. Geophysical Research* (in press).
12. N. Untersteiner and G.A. Maykut, "Arctic sea ice." *Naval Research Reviews*, p. 12-23, May 1969.
13. G.F.N. Cox and W.F. Weeks, *Brine Drainage and Initial Salt Entrapment in Sodium Chloride Ice*, 85 pp., CRREL Research Report 345, 1975.
14. K. Ahlnas and G. Wendler, "Arctic sea ice conditions in early spring viewed by satellite." *Arctic and Alpine Research*, **9**, 61-72, 1977.
15. W.I. Wittmann and J.J. Schule, "Comments on the mass balance of the arctic ice pack." *In* (J.O. Fletcher, ed.) *Proceedings of the Symposium on*

Digitized by Google

Original from
UNIVERSITY OF MICHIGAN

Generated for member (University of Maryland, College Park) on 2014-10-01 20:22 GMT / http://hdl.handle.net/2027/mdp.39015047405512
Public Domain, Google-digitized / http://www.hathitrust.org/access_use#pd-google

the Arctic Heat Budget and Atmospheric Circulation, p. 215-246, The RAND Corporation, RM-5233-NSF, 1966.

16. L.A. LeShack, W.D. Hibler, and F.H. Morse, "Automatic processing of arctic pack ice data obtained by means of submarine sonar and other remote sensing techniques." *In* (J.B. Lomax, ed.) *Propagation Limitations in Remote Sensing*, p. 5.1-5.14, NATO Publication AGARD-CP-90-71, 1971.

Sonar Technology Advanced at NCSL

Scientists and engineers at the Naval Coastal Systems Laboratory, Panama City, Flordia, achieved a milestone in synthetic aperture sonar technology recently when they successfully demonstrated reconstruction of a synthesized sonar beam which had been destroyed by adverse motions of the towed sonar vehicle.

According to task leader Frank Higgins, previous work at NCSL in synthetic aperture sonar technology had shown the feasibility of the vernier array synthetic aperture concept for high resolution beamforming when adverse motions of the sonar vehicle were not a factor in producing spurious phase errors that destroyed the synthesized beam. Any deviation of the sonar vehicle from a straight line, however, caused the image to be blurred. With the newly developed technology, the task team can measure the path of the vehicle and then correct the sonar data for it so that the sonar thinks it has flown a straight line.

The new technology builds on an earlier developmental phase of the synthetic aperture sonar at NCSL in 1975 which marked the first time synthetic aperture processing in sonar had been accomplished.

Because of sonar technology the ability to discern small underwater objects is determined by the length of the hydrophone array which a sonar system uses and to detect small objects at long ranges require an array many feet long, a small physical aperture or array was used to synthesize the required large aperture. They thus overcame the limitations of physical aperture sonar and became proficient in synthesizing a large aperture in the water by moving a small aperture along a line that would represent the length of the longer aperture if it were real. The sonar signals collected as the smaller aperture traveled through the water were stored in a computer memory so that all signals received by the small aperture became available for processing into the larger synthesized aperture.

The usefulness of the concept depended upon compensating motion-induced phase errors. This capability has now been successfully demonstrated.

The NSCL task team designed and built a sonar test vehicle incorporating state of the art technology, which is the application of microprocessors for control logic. The vehicle also contains an inertial measuring unit plus associated sonar and control logic electronics.

Digitized by Google

Original from
UNIVERSITY OF MICHIGAN

Generated for member (University of Maryland, College Park) on 2014-10-01 20:22 GMT / http://hdl.handle.net/2027/mdp.39015047405512
Public Domain, Google-digitized / http://www.hathitrust.org/access_use#pd-google

Research Notes

Dolphins in Sonar Studies

Working from Sea World, Orlando, Florida, Naval Research Laboratory scientists have recruited two Sea World dolphins, Guy and Mary, in a study to improve measurements of dolphin sonar signals. The investigators hope to obtain knowledge which may be used to improve naval sonar sytems.

Lynn Poche, principal investigator for the program, says dolphins have a remarkable active sonar system. They emit short pulses of sound which are reflected back to them by objects in the water, enabling them to locate food and avoid obstacles. In the dark depths of the ocean, where light and other electromagnetic waves cannot penetrate, sound is the best means of probing the environment.

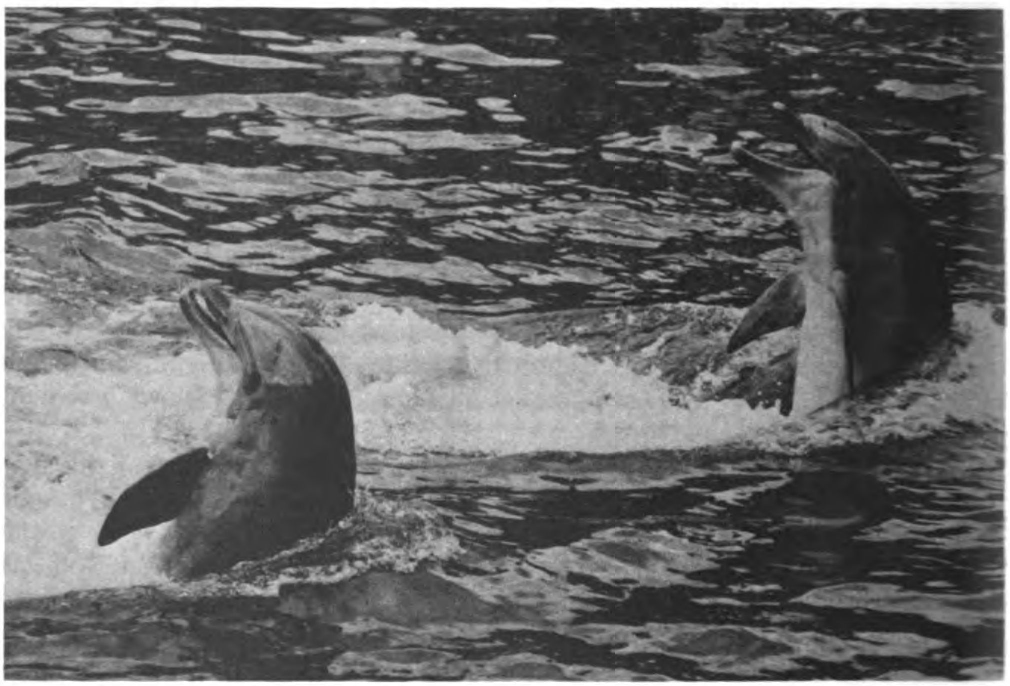

Guy and Mary, two Sea World dolphins, have signed up for a one-year temporary duty assignment. They're "sounding off" for the Naval Research Laboratory scientists in a study to improve measurements of dolphin sonar signals.

At Sea World experiments have been devised in which the bottlenose dolphins have to use their own sonar to make basic decisions, thus establishing a good source of representative signals for study and evaluation. Each dolphin records its determinations on selection paddles. The selection paddles provide the communication vehicle through which Guy and Mary are told if their selection is correct. The NRL scientists hope to gather more precise data on dolphin sonar, and develop new techniques in their study by careful measurement and analysis of the dolphins' signals.

U. S. GOVERNMENT PRINTING OFFICE : 1978 O - 272-889

Digitized by Google
Original from UNIVERSITY OF MICHIGAN
Generated for member (University of Maryland, College Park) on 2014-10-01 20:22 GMT / http://hdl.handle.net/2027/mdp.39015047405512
Public Domain, Google-digitized / http://www.hathitrust.org/access_use#pd-google

Studying dolphin sonar is not new. Many years of research have been devoted to dolphin studies at other places such as the Naval Oceans System Center in Hawaii, and San Diego, Ca. and Woods Hole Oceanographic Institution, Mass.

"We're using Guy and Mary as sound producers," says Poche. "But it's much more than that. Their biological sonar is so efficient that we study it to improve ours."

Formation of the Bioelectromagnetic Society

Dr. Thomas C. Rozzell Project Officer, Electromagnetic Radiation Effects, ONR, has just completed the initial steps in the formation of the Bioelectromagnetics Society. It is a society whose purpose is to foster and encourage research involving the interaction of electromagnetic energy and biological systems. The Society while based in North America will be international in scope and will embrace many different disciplines and a number of areas of research including the effects of electromagnetic fields, the therapeutic and diagnostic uses, the analytic uses, and the uses of electromagnetic fields by biological organisms in their normal habitats. The growth of the bioelectromagnetics research community over the past few years has been nothing less than phenomenal and the prediction for the future is that this rate of growth will continue to increase. The need for the Society was thus dictated by the sheer number of persons involved and the fact that no single current society addresses the myriad spectrum of problems and concerns of this research group. Today there is no central focus for dissemination of information and no central journal to publish the growing number of papers emanating from this research. When the society becomes better established it will try to remedy these probems. Those wishing more information should write to The Bioelectromagnetics Society, P.O. Box 3651, Arlington, VA 22203.

NAVAL RESEARCH REVIEWS publishes highlights of research conducted by Navy laboratories and contractors and describes important naval experimental facilities. Manuscripts submitted for publication, correspondence concerning prospective articles, and changes of address, should be directed to Code 730, Office of Naval Research, Arlington, Va. 22217. Requests for subscriptions should be directed to the Superintendent of Documents, U.S. Government Printing Office, Washington, D.C., 20402. Subscription price: $6.50 per year in the U.S. and Canada; $8.15 per year, foreign; $0.55 per individual copy. The issuance of this periodical approved in accordance with Dept. of the Navy publications and printing regulations.

Editor: WILLIAM J. LESCURE NAVSO P-510

Associate Editors:

L. LARMORE, ONR PASADENA
G. SANDOZ, ONR CHICAGO
A.L. POWELL, ONR BOSTON
D.A. PATTERSON, NAVAL RESEARCH LABORATORY

Generated for member (University of Maryland, College Park) on 2014-10-01 20:22 GMT / http://hdl.handle.net/2027/mdp.39015047405512
Public Domain, Google-digitized / http://www.hathitrust.org/access_use#pd-google

Digitized by Google

Original from
UNIVERSITY OF MICHIGAN

IN THIS ISSUE

VOL. XXXI, NO. 7

A review is presented here of the applications of variable camber to enhance maneuverability on contemporary combat aircraft, especially increased transonic maneuverability and off design performance.

The calculations related to this research suggest that the interaction between atmosphere and ocean in the presence of a dynamic ice cover is more vigorous than previously believed.

Cover Caption

An artist's concept of U.S. Navy F-18 aircraft which is being designed to exploit variable camber for improved maneuverability. The F-18 system will be automatic and follows a complex deployment schedule. *See article on page 1.* -

---

DEPARTMENT OF THE NAVY
OFFICE OF NAVAL RESEARCH
ARLINGTON, VA. 22217

OFFICIAL BUSINESS

PENALTY FOR PRIVATE USE, $300.

POSTAGE AND FEES PAID
DEPARTMENT OF THE NAVY
DoD-316
CONTROLLED CIRCULATION RATE

U.S.MAIL

Generated for member (University of Maryland, College Park) on 2014-10-01 20:22 GMT / http://hdl.handle.net/2027/mdp.39015047405512
Public Domain, Google-digitized / http://www.hathitrust.org/access_use#pd-google

Digitized by Google

Original from
UNIVERSITY OF MICHIGAN